Supporting Information for: Metallopeptide-Based Mimics Suggest Substrate Orientation Directs Sulphur Oxidation vs Hydrogen Atom Abstraction Reactions in Mononuclear Non-Haem Iron Dioxygenases

Jason Shearer,* Sara Bassiri, Kendal Southwell, and Dovydas Vasiliauskas

Department of Chemistry, Trinity University, San Antonio, TX 78212, USA

E-mail: jshearer@trinity.edu

Table of Contents

Materials, Method and Additional Results

Generation of Metallopeptides. High purity peptides (purity > 98%) nh1 (HCDLPHA) and nh2 (HHDLPCA) were obtained from GenScript custom peptide synthesis, and were used as received following an assessment of their purity and composition by LC/MS (Figures S1 – S3). Both ESI-MS and gel-permeation chromatography (GPC) studies indicate the lack of intermolecular disulphide bonds have formation. Peptide solutions were generated and manipulated in a COY anoxic chamber under an atmosphere of 97:3 N_2:H_2 at a pH = 8.0 maintained using a 50 mM NEM buffer. Water used to generate all solutions was purified to a resistance of at least 18 MΩ·cm. All peptide concentrations were determined using an Ellman's assay.[1]

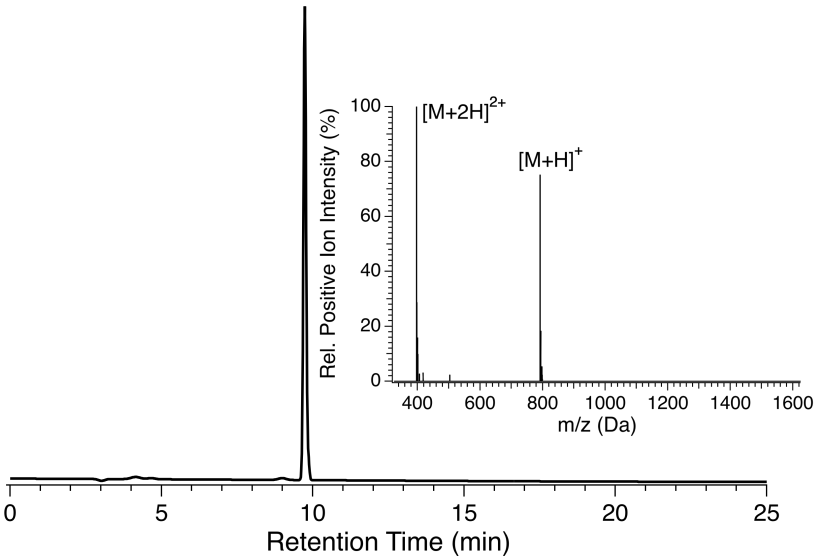

Figure S1. HPLC (left) and positive ion-mode ESI-MS (right) of nh1. LC/MS data were obtained on an Agilent 6230 Electrospray Ionization Time-of-Flight Mass Spectrometer with an Agilent 1260 Infitinty II HPLC equipped with a Waters XTerra C-18 analytical column (4.6 × 150 mm; 5 μm). A linear gradient of 10 - 65% MeCN in water (0.1% formic acid) over 25 min was used.

The stoichiometry between Fe^{2+} and peptides were obtained using electronic absorption spectroscopy on a JASCO V730 UV/Vis-NIR spectrometer house in a COY chamber. Aliquots of ferrous chloride tetrahydrate in water (50 mM stock solution) were added to

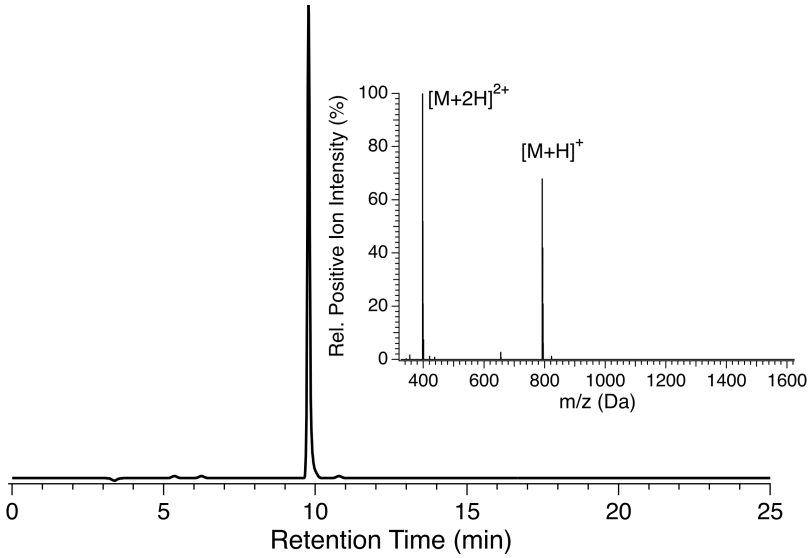

Figure S2. HPLC (left) and positive ion-mode ESI-MS (right) of nh2. LC/MS data were obtained on an Agilent 6230 Electrospray Ionization Time-of-Flight Mass Spectrometer with an Agilent 1260 Infitinty II HPLC equipped with a Waters XTerra C-18 analytical column (4.6 × 150 mm; 5 μm). A linear gradient of 10 - 65% MeCN in water (0.1% formic acid) over 25 min was used.

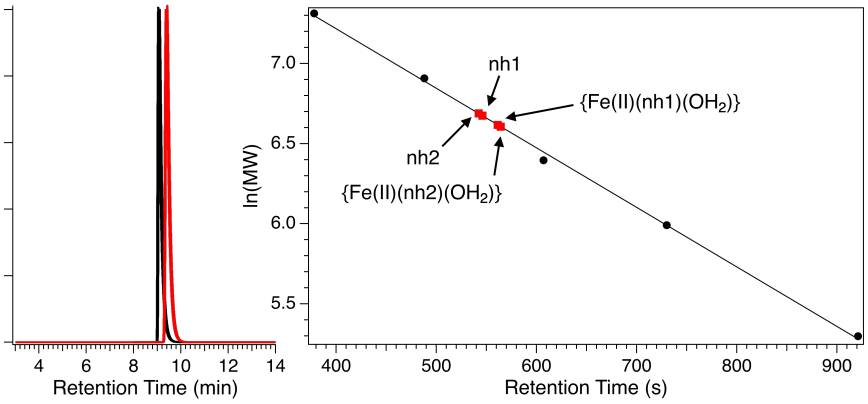

Figure S3. Representative GPC results obtained on a Waters DeltaPrep 60 Waters HPLC system equipped with a Protein-Pak GPC column (7.8 × 300 mm, 60 Å pore size) using an aqueous solution of $NaHCO_3$ (sat.) under a positive pressure of He(g). Poly(ethylene glycol) standards were purchased from Waters. Left: GPC chromatograms of nh1, nh2, {Fe(II)(nh1)(OH_2)} and {Fe(II)(nh2)(OH_2)}. The two peptide are the black traces and the two metallopeptides are the red traces. Right: Calibration curve and individual retention times of poly(ethylene glycol) standards (black line and circles). The red squares are the retention times of nh1, nh2, {Fe(II)(nh1)(OH_2)} and {Fe(II)(nh2)(OH_2)}. The retention times for nh1, nh2, {Fe(II)(nh1)(OH_2)} and {Fe(II)(nh2)(OH_2)} indicate they are monomeric in nature and that the metallopeptides have a lower apparent MW. The lower apparent MW by GPC is a result of the peptide backbone wrapping about the Fe(II) centre, which yields a more compact structure than the free peptide, and hence a longer retention time.

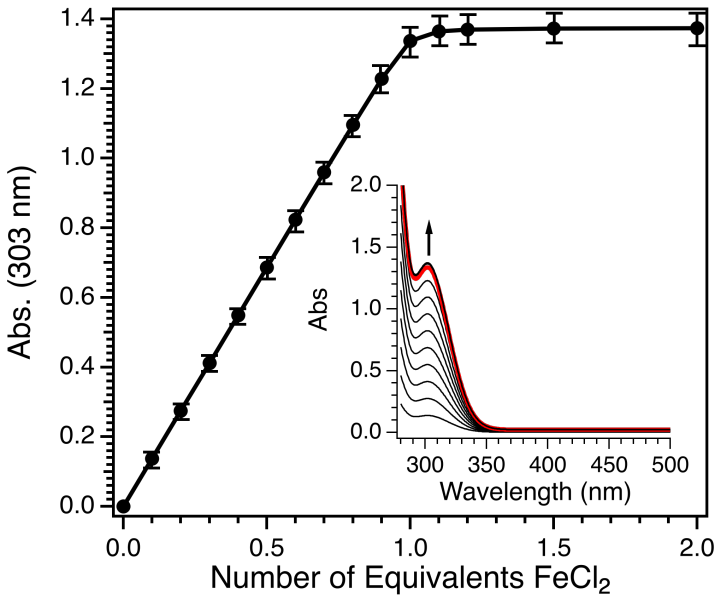

Figure S4. Room temperature titration of $FeCl_2$(aq) into 1.0×10^{-3} M nh1 solutions at a pH = 8.0 (50 mM NEM buffer solution) showing the increase of the 304 nm CT band upon increasing Fe(II) concentration. The inset shows the individual UV/vis trances. The red trace corresponds to a 1:1 Fe(II):nh1 molar ratio. The standard error for each data point is based on three separate titrations on independently prepared peptide solutions.

peptide solutions of 1 mM or less, yielding titration plots outlined in Figures S1 (Fe^{2+} + nh1) and S2 (Fe^{2+} + nh2) while monitoring the increase of the intensity of the lower-energy LMCT band at $\sim$ 305 nm. All titrations were performed in triplicate. Based on fitting the titration data Fe(II) K_d values of $< 2\mu$M were obtained for both {Fe(II)(nh1)(OH_2)} and {Fe(II)(nh2)(OH_2)}. GPC studies of {Fe(II)(nh1)(OH_2)} and {Fe(II)(nh2)(OH_2)} (generated by the addition of 1.0 eq of $FeCl_2$ to nh1/2 solutions at pH = 8.0 (50 mM NEM buffer)) were performed in an anerobic bag under a continuous Ar(g) purge, and indicate a 1:1 Fe(II):peptide stoichiometry.

All subsequent metallopeptide solutions were made by injecting 1.0 eq of Fe^{2+} (from the above 50 mM stock solution) into solutions of nh1 or nh2 at pH = 8.0 (50 mM NEM buffer). Electronic absorption spectra were recorded on an Agilent CARY 5000 UV/Vis-NIR spectrometer and circular dichorism (CD) spectra were recorded on a JASCO J1500 spectropolarimeter (Figure S3). Optical spectra were obtained at room temperature in sealed

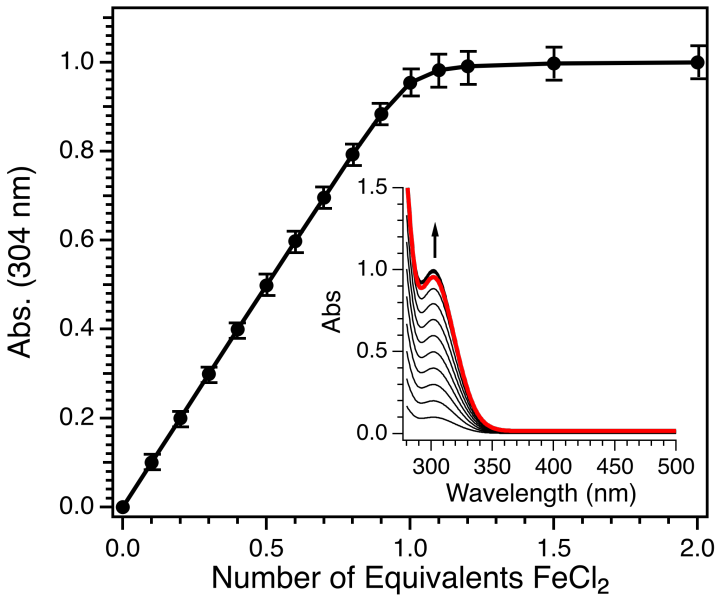

Figure S5. Room temperature titration of $FeCl_2$(aq) into 7.5×10^{-4} M nh2 solutions at a pH = 8.0 (50 mM NEM buffer solution) showing the increase of the 303 nm CT band upon increasing Fe(II) concentration. The inset shows the individual UV/vis traces. The red trace corresponds to a 1:1 Fe(II):nh2 molar ratio. The standard error for each data point is based on three separate titrations on independently prepared peptide solutions.

air-free 1 cm rectangular cuvettes. CD data represent the summed average of ten individual spectra.

Oxidation reactions were performed by exposing pH 8.0 (50 mM NEM) solutions of {Fe(II)(nh1)(OH_2)} or {Fe(II)(nh2)(OH_2)} to O_2 or $^{18}O_2$ (ICON isotopes). Upon exposure of reduced peptide solutions to dioxygen an immediate color change from a colorless to rust-colored orange solution was noted followed by the formation of a brownish-red colored solid. The oxidation reactions were then filtered through nylon membranes (0.45 μm pore size) resulting in clear colorless solutions which were analyzed by LC/MS on an Agilent 6230 Electrospray Ionization Time-of-Flight Mass Spectrometer with an Agilent 1260 Infitinty II HPLC equipped with a Waters XTerra C-18 analytical column (4.6 × 150 mm; 5 μm). A linear gradient of 10 - 25% MeCN in water (0.1% formic acid) over 25 min was used (Figure 6 of the main manuscript and Figures S14 – S17). MALDI-TOF mass spectrometry of the solids generated in the above reactions (Figures S20 and S21) were performed using CHCA

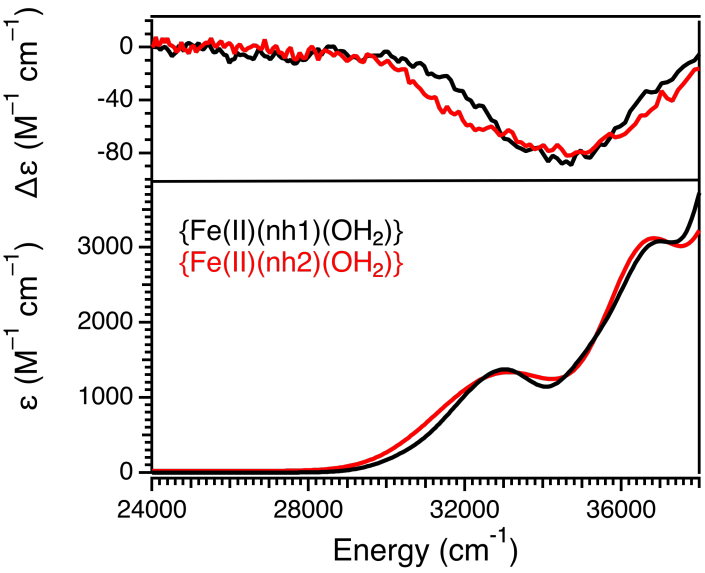

Figure S6. Electronic absorption (bottom) and CD spectra (top) recorded for {Fe(II)(nh1)(OH_2)} (black) and {Fe(II)(nh2)(OH_2)} (red) at room temperature (pH 8.0 50 mM NEM buffer).

as the matrix material on a Bruker MicroFlex MALDI-TOF in positive ion mode.

Iron K-edge X-ray Absorption Spectroscopy. Reduced metallopeptide solutions were prepared in a COY chamber at a concentration of 2.0 mM in a 4:1 mixture of 50 mM NEM buffer pH 8.0:glycerol, injected into lucite sample holders with windows of Kapton tape and quickly frozen in liquid nitrogen. Data were collected at the Stanford Synchrotron Radiation Laboratory (Menlo Park, CA) on beamline 7-3 at 12(2) K with temperatures maintained using an Oxford liquid He cryostat. Light was monochromatized using a Si(220) double crystal monochromator, which was detuned 50% for harmonic rejection. Spectra were obtained in fluorescence mode using a 30-element solid-state Ge detector (Canberra) with an manganese filter placed between the sample and detector. Spectra were calibrated against the first inflection point of Fe-foil (7111.2 eV), which was simultaneously recorded with the samples. Data were obtained in 10 eV steps in the pre-edge region (6912 – 7092 eV, 1 s integration time), 0.3 eV steps in the pre-edge region (7092 – 7135 eV, 2 s integration time), 1.0 eV steps in the edge region (7135 – 7155 eV, 2 s integration time), 2.0 eV steps in the near edge region (7155 – 7455 eV, 3 s integration time), and 0.05 k steps in the far edge region

(7455 eV – 15.0 $Å^{-1}$, 3 s integration time). Although no photodamage was noted from scan to scan, the 1 × 5 mm beam spot was moved after every 2 scans. Total fluorescence counts were maintained under 30 kHz, and a deadtime correction yielded no appreciable change to the data. The reported spectra represent the averaged spectra from 8 individual data sets. Prior to data averaging each spectrum and detector channel was individually inspected for data quality. Although data were recorded to 15 $Å^{-1}$, the data were analyzed only to 14.3 $Å^{-1}$ owing to noise at high k. Data were subsequently processed and analyzed as previously reported using EXAFS123 and FEFF 9.4 as previously reported[2] except for further processes of the pre-edge features (see below). Errors to the EXAFS models are reported as ϵ^2 values.[3]

The individual transitions comprising the pre-edge peaks were extracted as follows. Following removal of the edge jump the pre-edge was modeled as three pseudo-Voigt line shapes (1:1 mixture of Gaussian:Lorentzian functions). Owing to the fact that multiple minima could be located if peak intensity, energy and line-widths were permitted to freely float the fwhm for all three peaks were restrained to 1.1 eV and the second highest energy transition was restrained to have an intensity greater than 0 but less than the highest energy transition. Extraction of excitation energies led to the $10Dq$ and B values for {Fe(II)(nh1)(OH_2)} and {Fe(II)(nh2)(OH_2)} listed in Table S4.

Iron L-edge X-ray Absorption Spectroscopy. Thin films of {Fe(II)(nh1)(OH_2)} and {Fe(II)(nh2)(OH_2)} were prepared by the slow evaporation of a 20 μL volume of metallopeptide solution ($\sim$ 0.5 mM) placed on a 7.0 × 5.0 mm silicon wafers (SPI Supplies) under an Ar atmosphere. Data were collected at the National Synchrotron Light Source II (Upton, NY) on beamline 23-ID-2 in as total fluorescence yield data. Data were collected in 0.4 eV steps prior to the Fe L_3 edge (660 - 700 eV) 0.1 steps in the L_3 and L_2 edge region (700 - 730 eV) and the 0.4 eV steps past the L_2 edge region (730 - 850 eV). Data were collected on multiple metallopeptide thin films and represent the average of 10 spectra. Following data averaging a baseline was fit to the data by modeling the background as a polynomial function before the L_3 edge and then modeling the edge jumps as:

Table S1. Reported fit and alternative models for the EXAFS data obtained for {Fe(II)(nh1)(OH_2)}. $E_o = 7122.6$ eV for all fits.

	$\mathbf{N_4OSIm_2(a)}$	$\mathbf{N_4OSIm_2(b)}$	$\mathbf{N_4OS}$	$\mathbf{N_5SIm_2}$[a]	$\mathbf{N_5S}$	$\mathbf{N_6}$
Fe-S Shell						
n	1	1.0(8)	1	1	1	–
r (Å)	2.391(15)	2.39(7)	2.390(7)	2.396(4)	2.385(4)	
σ^2 (Å^2)	0.0013(3)	0.0014(13)	0.0021(6)	0.0013(4)	0.0033(4)	
Fe-N Shell						
n	4	4.0(6)	4	5	5	6
r (Å)	2.165(3)	2.165(10)	2.165(5)	2.169(4)	2.167(4)	2.165(2)
σ^2 (Å^2)	0.0033(6)	0.0033(14)	0.0049(13)	0.0049(6)	0.0041(6)	0.0059(3)
Fe-O Shell						
n	1	1.0(6)	1	–	–	–
r (Å)	2.292(4)	2.202(5)	2.29(2)			
σ^2 (Å^2)	0.0020(5)	0.0020(13)	0.0020(11)			
Fe-Im Shell[b]						
n	2	2.6(8)	–	2	–	–
r (Å)	2.1650	2.1650		2.1692		
σ^2 (Å^2)	0.006(4)	0.006(3)		0.002(2)		
θ (°)	18.4(80)	18.4(50)		14(2)		
r' (Å)	0.0(4)	0.0(10)		0.7(45)		
ϵ^2	0.57	0.54	0.66	0.58	0.66	1.00

[a] **Reported fit**. Although ϵ^2 is slightly higher for this fit than the N_4SOIm_2 fit we report this model as it is both statistically valid (ϵ^2 is within 1.0 of the lowest achievable value) and the separation of the N and O shells are not justified at this resolution of data ($\Delta r > 0.15$ Å based on $\Delta k = 12.1$ Å^{-1}).

[b]This shell only included contributions to the imidazole outersphere single and multiple scattering pathways. The innersphere pathway was included with the Fe-N single scattering pathways. The distance variable refers to the innersphere Fe-N distance and was restrained to the value obtained from the Fe-N single scattering pathway. We note that the values of θ and r', which describe the deviation of the Fe atom out-of-plane with respect to the imidazole ring (r') and the angle of inflection of the iron atom out-of-plane with respect to the imidazole ring (θ), has no real physical meaning when the number of imidazoles considered is greater than one.

Table S2. Reported fit and alternative models for the EXAFS data obtained for {Fe(II)(nh2)(OH_2)}. $E_o = 7122.9$ eV for all fits.

	$\mathbf{N_4OSIm_2(a)}$	$\mathbf{N_4OSIm_2(b)}$	$\mathbf{N_4OS}$	$\mathbf{N_5SIm_2}$[a]	$\mathbf{N_5S}$	$\mathbf{N_6}$
Fe-S Shell						
n	1	0.93(11)	1	1	1	–
r (Å)	2.39(2)	2.40(5)	2.38(2)	2.338(10)	2.324(13)	
σ^2 (Å^2)	0.0020(4)	0.004(6)	0.0016(3)	0.0029(12)	0.0011(2)	
Fe-N Shell						
n	4	5.6(6)	4	5	5	6
r (Å)	2.166(3)	2.168(10)	2.165(3)	2.168(3)	2.163(3)	2.161(2)
σ^2 (Å^2)	0.0017(3)	0.0042(15)	0.0021(4)	0.0044(3)	0.0056(3)	0.0057(2)
Fe-O Shell						
n	1	0.8(2)	1	–	–	–
r (Å)	2.301(3)	2.308(15)	2.309(4)			
σ^2 (Å^2)	0.0028(3)	0.007(3)	0.0024(4)			
Fe-Im Shell[a]						
n	2	1.8(6)	–	2	–	–
r (Å)	2.1656	2.1680		2.1677		
σ^2 (Å^2)	0.007(3)	0.004(6)		0.0010(6)		
θ (°)	17.6(3)	18.7(3)		18(3)		
r' (Å)	0(6)	0.4(12)		0(2)		
ϵ^2	0.61	0.56	0.77	0.68	0.75	1.02

[a] **Reported fit**. Although ϵ^2 is slightly higher for this fit than the N_4SOIm_2 fit we report this model as it is both statistically valid (ϵ^2 is within 1.0 of the lowest achievable value) and the separation of the N and O shells are not justified at this resolution of data ($\Delta r > 0.15$ Å based on $\Delta k = 12.1$ Å^{-1}).

[b]This shell only included contributions to the imidazole outersphere single and multiple scattering pathways. The innersphere pathway was included with the Fe-N single scattering pathways. The distance variable refers to the innersphere Fe-N distance and was restrained to the value obtained from the Fe-N single scattering pathway. We note that the values of θ and r', which describe the deviation of the Fe atom out-of-plane with respect to the imidazole ring (r') and the angle of inflection of the iron atom out-of-plane with respect to the imidazole ring (θ), has no real physical meaning when the number of imidazoles considered is greater than one.

$$I_n = H_n\left(\frac{1}{2} + \pi^{-1}\arctan\left[\frac{E - P_n}{0.5\Gamma}\right]\right) \quad (1)$$

where n = 2 or 3, H_n is the height of the L_n edge, P_n is the energy of the L_n edge and Γ is the width of the jump. Data were subsequently modeled within a ligand-field multiplets framework using the software package *CT4XAS*.[4] Data were modeled using an O_h ligand field without the need for included charge-transfer effects (Figure S4). For these calculations the appropriate Slater integrals were reduced to 90% of their atomic values for {Fe(II)(nh1)(OH_2)} and 80% of their atomic values for {Fe(II)(nh2)(OH_2)}, while core and valence spin orbit coupling values were reduced to 90% of their atomic values for both complexes. The value for $10D_q$ used in the crystal field model were 0.94 eV for {Fe(II)(nh1)(OH_2)} and 0.99 eV for {Fe(II)(nh2)(OH_2)}, which are in-line with the AILFT values derived below. Spectral line shapes were simulated by application of pseudo-Voight functions to each transition and summing the individual transitions (line broadening: Gaussian *fwhm* = 0.20 eV; Lorentzian *fwhm* = 0.20 eV below 715 eV and 0.50 eV above 715 eV).

Sulfur K-edge X-ray Absorption Spectroscopy. Reduced metallopeptide solutions were prepared in a COY chamber at a concentration of 2.0 mM in a 4:1 mixture of 50 mM NEM buffer pH 8.0:glycerol, injected into aluminum sample holders with windows made from 2.5 μm thick Mylar film and quickly frozen in liquid nitrogen. Sample oxidation was achieved by allowing the samples to warm to room temperature in air and then immediately refreezing the sample in liquid nitrogen. Data were collected at the Stanford Synchrotron Radiation Laboratory (Menlo Park, CA) on beamline 4-3 in a He(g) atmosphere. Samples were maintained at $\sim$ 100 K using a cold He(g) cryostream positioned directly over the sample. Light was monochromatized using a Si(111) double crystal monochromator, which was detuned 75% for harmonic rejection, and data were collected in fluorescence mode using a 4-element Si-drift detector. The energy was calibrated to the first inflection point of a sample of $Na_2S_2O_3$ (2472.02 eV) collected before and after sample data collection; no drift in energy was noted during data collection. Spectra were obtained in 1.0 eV steps in the

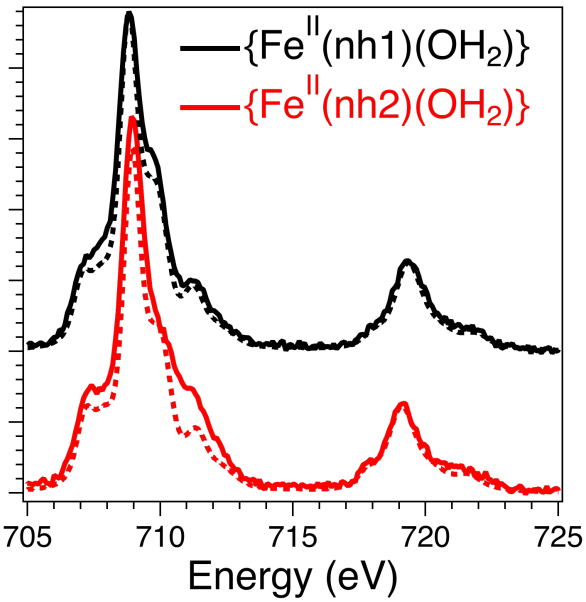

Figure S7. Fe L-edge XAS spectra following baseline subtraction for {Fe(II)(nh1)(OH_2}} (black spectrum) and {Fe(II)(nh2)(OH_2}} (red spectrum). The experimental data are depicted as the solid spectra and the best fits to the experimental data are depicted as the dashed spectra.

pre-edge region (2365 - 2465 eV; 1 s integration time) 0.1 eV steps in the edge region (2465 - 2485 eV; 2 s integration time) and 2.0 eV steps in the post edge region (2485 - 2700 eV; 2 s integration time). The reported data represent the average of five scans. Data were subsequently worked-up and analyzed as previously reported using [Et_4N]($FeCl_4$) as an Fe-S covalency standard.[5]

Electronic Structure Calculations. Electronic structure calculation were performed using the electronic software suite *ORCA* v. 5.0.3 or 6.0.1.[6] All calculations employed the def2-tzvp basis set on all atoms and "tightscf" convergence criteria. Geometry optimizations employed the BP86 density functional followed by the PBE0 hybrid density functional, the atom-pairwise dispersion correction with Becke-Johnson damping (D3), and the conductor-like polarization model with parameters appropriate for water (cpcm(water)). Starting atomic coordinates for these geometry optimizations were constructed from the crystallographic coordinates for the nickel center and the first six residues (HCDPLC) from the *Streptomyces seoulensis* NiSOD protein structure (PDB ID = 1Q0D) with the following

modifications: a) H-atoms were placed in idealized positions, b) the Ni(III) center was replaced with an Fe(II) center, c) the side chain of D3 was replaced with a hydrogen atom, d) either C6 was changed to H (nh1 computational mimic) or C2 was changed to H (nh2 computational mimic) , and e) a water was placed *trans* to the coordinate imidazole ligand from H1. Oxidized Fe(III) models were generated in an identical manner except that the water molecule was replaced with an O_2^- ligand. For the oxidized Fe(III)superoxo-bound models the broken symmetry approximation was used to account for spin-coupling between the unpaired spins on the superoxo-ligand and the iron-center. Magnetic exchange constants, J, were calculated using the formalism of Soda and co-workers.[7] Single point calculations were performed on these geometry optimized structures using the same methods as above using the PBE0 hybrid density functional. Orbital populations are reported as Löwdin populations. Isosurface plots were generated using the *UCSF Chimera* visualization software package.[8]

Table S3. Calculated Fe-ligand bond lengths (Å) from the PBE0/def2-tzvp/D3/CPCM(water) geometry optimization calculations.

	Fe(II)nh1(OH_2)	Fe(II)nh2(OH_2)	Fe(III)nh1(O_2^-)	Fe(III)nh2(O_2^-)
Fe-S	2.366	2.379	2.248	2.239
Fe-N (axial)	2.150	2.113	2.042	2.042
Fe-N (amine)	2.255	2.230	2.016	2.006
Fe-N (amide)	2.104	2.131	1.916	1.968
Fe-N (imidazole)	2.179	2.139	2.071	1.959
Fe-OH_2	2.335	2.370	—	—
Fe-ceO2-	—	—	1.827	1.854

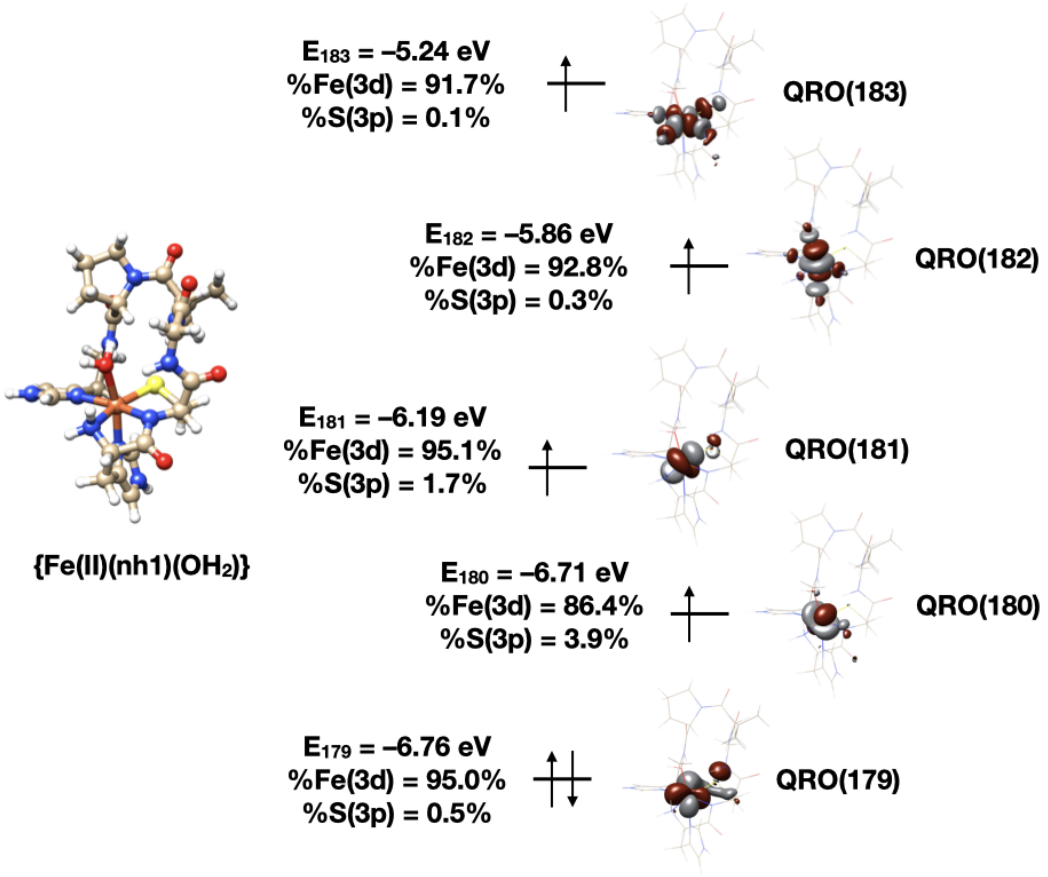

Figure S8. Left: Ball and stick representation of the geometry optimized structure of {Fe(II)(nh1)(OH_2)} (PBE0/def2-tzvp/D3/cpcm(water)). Right: Isosurface plots of the quasirestiricted orbitals (QROs; 0.03 a.u.) corresponding to the nominal 3d-orbitals for {Fe(II)(nh1)(OH_2)} along with calculated QRO energies and Fe(3d) and S(3p) AO compositions to the QROs (Löwdin populations).

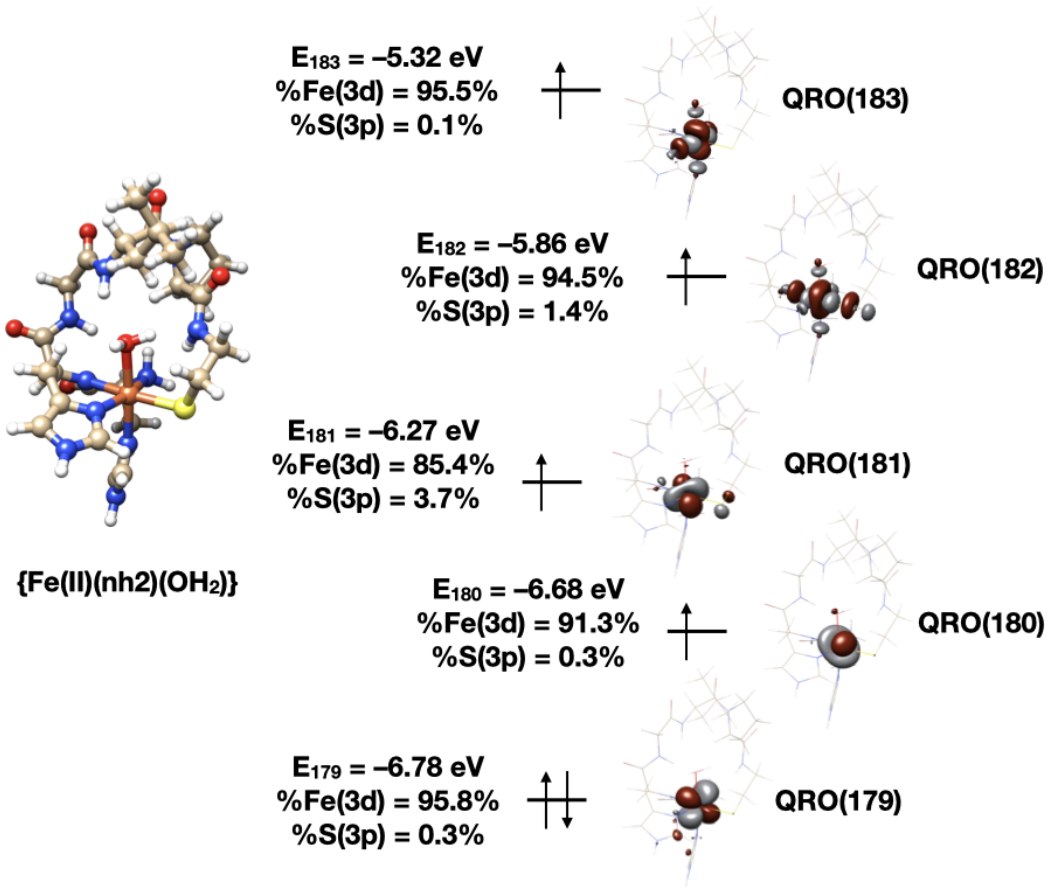

Figure S9. Left: Ball and stick representation of the geometry optimized structure of {Fe(II)(nh2)(OH_2)} (PBE0/def2-tzvp/D3/cpcm(water)). Right: QROs (0.03 a.u.) corresponding to the nominal 3d-orbitals for {Fe(II)(nh2)(OH_2)} along with calculated QRO energies and Fe(3d) and S(3p) AO compositions to the QROs (Löwdin populations).

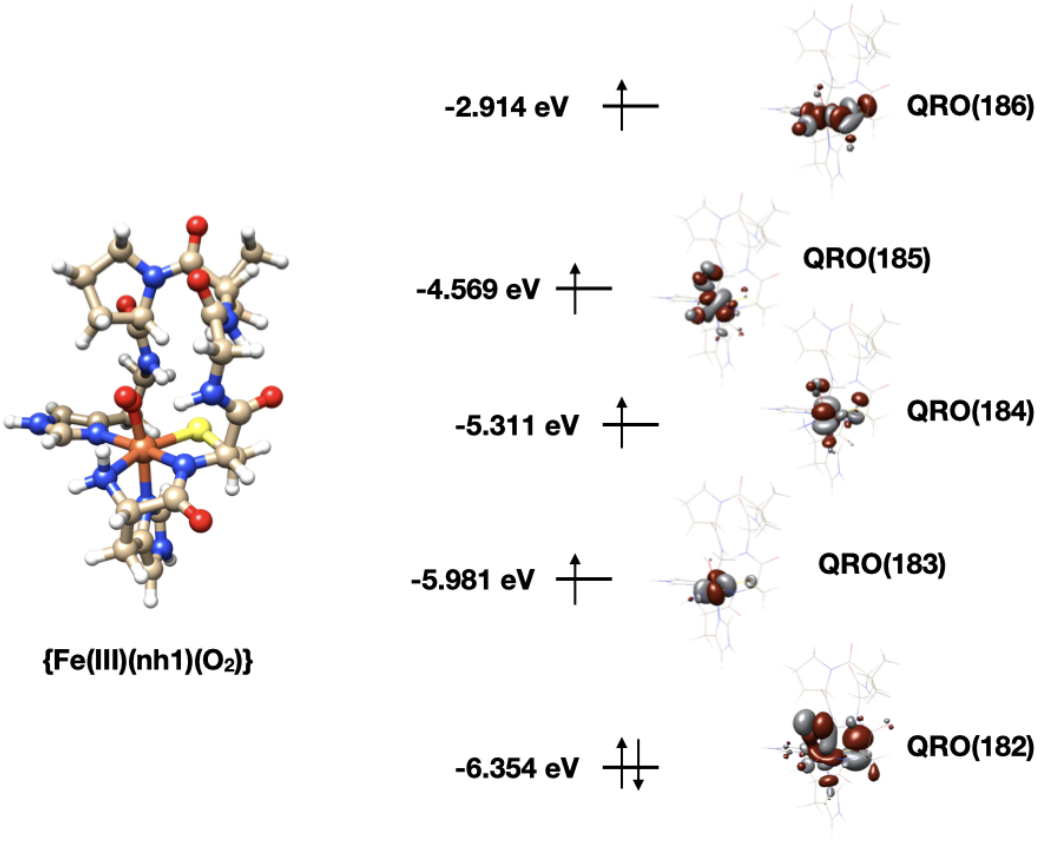

Figure S10. Left: Ball and stick representation of the geometry optimized structure of {Fe(III)(nh1)(O_2)} (PBE0/def2-tzvp/D3/cpcm(water)). Right: QROs (0.03 a.u.) corresponding to the nominal 3d-orbitals for {Fe(III)(nh1)(O_2)}.

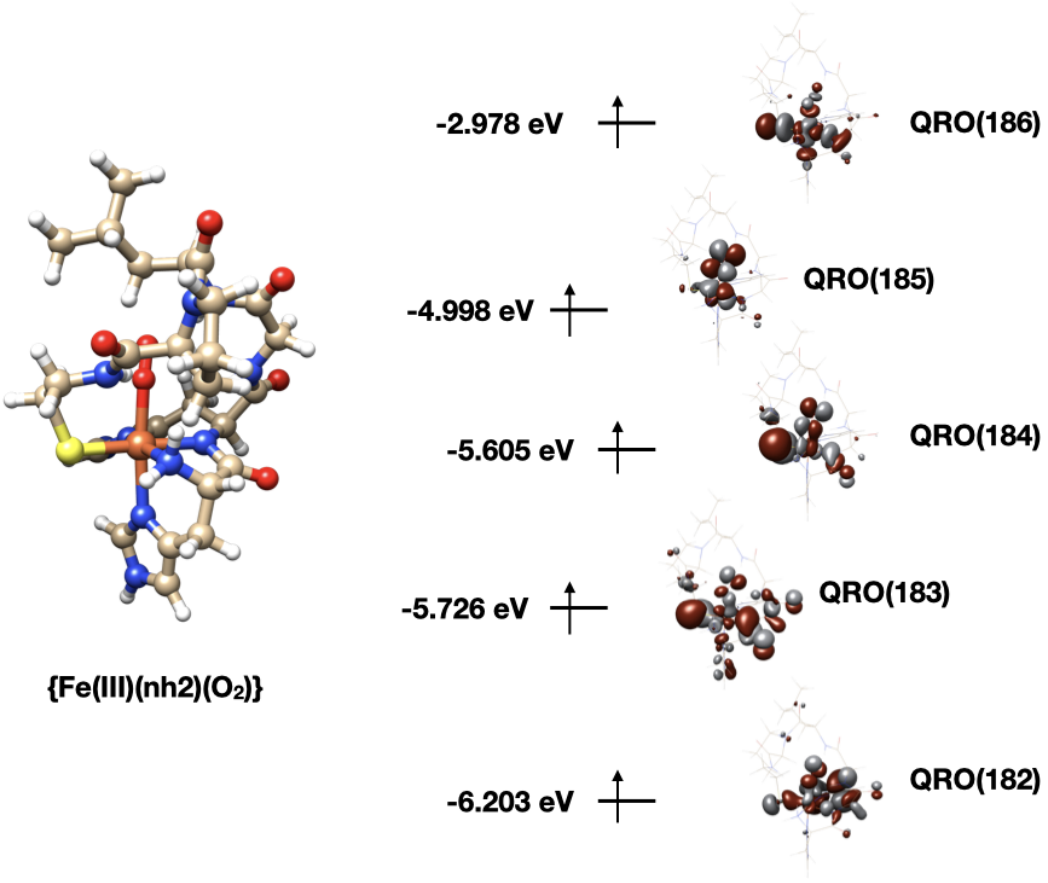

Figure S11. Left: Ball and stick representation of the geometry optimized structure of {Fe(III)(nh2)(O_2)} (PBE0/def2-tzvp/D3/cpcm(water)). Right: QROs (0.03 a.u.) corresponding to the nominal 3d-orbitals for {Fe(III)(nh2)(O_2)}.

Ab Initio Ligand Field Theory and Subsequent Fe K-edge 1s→3d Multiplet Analysis

The reproduction of the pre-edge feature found in the Fe K-edge XANES spectra of {Fe(II)(nh-1)(OH_2)} and {Fe(II)(nh2)(OH_2)} utilized a Multiplets analysis with input parameters obtained from *ab initio* ligand field theory (AILFT) calculations of minimized metallopeptide models. All heavy atoms except the iron-center, oxygen from the coordinated water, and atoms from the side chains and backbone chelate were deleted from the full length peptide mimics. The appropriate hydrogen atoms were then added to the model, who's positions were then optimized at the PBE0/def2-tzvp/D3/cpcm(water) level of theory (all heavy atoms coordinates were restrained) resulting in the minimized metallopeptide models outlined in Figures S9 and S11.

All AILFT calculations were performed on these models using the SC-NEVPT2 method with def2-tzvp basis set and def2-tzvp/c auxiliary basis set. For the $3d^6$ Fe(II) ground state excitations among the purified d-orbitals on the quintet, triplet and singlet surfaces were examined by fully saturating the acceptor space (five roots on the quintet surface, 45 roots on the triplet surface, and 50 roots on the singlet surface). Solomon and co-workers have previously demonstrated that the final states for 1s→3d transitions can be modeled in such a manner as the increase in $Z_{\text{eff.}}$ following generation of a M(1s) hole is effectively mimicked as a Z+1 "excited state." Therefore, the excited states were modeled a $3d^7$ Co(II) with the iron center replaced by cobalt in the above models (all atom positions restrained to their Fe minimized positions). We examined excitations on the quartet and doublet surfaces with the acceptor spaces fully saturated (ten roots on the quartet surface and forty roots on the doublet surface). The results from these ground and excited state calculations are reported in Table S3. In addition, the K-edge transitions were also simulated using 2-shell AILFT (1s3d shells) examining all quintet, triplet and singlet surfaces transitions.

The d^7 Tanabe-Sugano matrices were also used to estimate the energies and intensities of

the final state transitions using the calculated values for $10D_q$, B and C were taken from the Co(II) AILFT calculations resulting in the values displayed in Table S4. Pre-edge peaks were then simulated by applying a pseudo-Voigt line shape (50/50 Gaussian/Lorentzian shape) to each transition with a 1.4 eV peak-width and summing the individual peaks (Figure S10/12). A comparison between the simulated pre-edge derived from O-symmetry and the 2-shell AILFT calculated pre-edge features are provided.

Table S4. AILFT results for the minimized metallopeptide computational mimics. All energies are given in eV. Also provided are $10D_q$ and B values obtained from fitting the pre-edge peaks from the Fe K-edge XAS data.

	{Fe(II)(nh1)(OH_2)}	{Co(II)(nh1)(OH_2)}	{Fe(II)(nh2)(OH_2)}	{Co(II)(nh2)(OH_2)}
$E(3d_1)$	0.000	0.000	0.000	0.000
$E(3d_2)$	0.092	0.087	0.114	0.118
$E(3d_3)$	0.132	0.127	0.232	0.229
$E(3d_4)$	0.873	0.826	0.884	0.822
$E(3d_5)$	1.248	1.191	1.336	1.278
$10D_q$[a]	0.986 (0.99)	0.937	0.995 (0.94)	0.934
B[a]	0.121 (0.12)	0.128	0.121 (0.12)	0.130
C/B	3.708	3.829	3.726	3.793

[a] Experimentally derived values are in the parenthasies.

Table S5. Calculated energies, populations and intensities of the Fe K-edge transitions from a Tanabe-Sugano analysis. The $^4A_1$ transitions have been omitted form this analysis since they result from double excitations, and would thus have no appreciable contribution towards the pre-edge feature.

Final State	{Fe(II)(nh1)(OH_2)}	{Fe(II)(nh2)(OH_2)}
$\underline{^4T_1(\mathrm{a})}$		
Hole Character	$0.097\|t_2^2e\rangle + 0.903\|t_2e^2\rangle$	$0.098\|t_2^2e\rangle + 0.902\|t_2e^2\rangle$
Relative Energy (eV)	0.0	0.0
Relative Intensity	1.903	1.902
$\underline{^4T_2}$		
Hole Character	$\|t_2^2e\rangle$	$\|t_2^2e\rangle$
Relative Energy (eV)	0.805	0.802
Relative Intensity	1.000	1.000
$\underline{^4T_1(\mathrm{b})}$		
Hole Character	$0.903\|t_2^2e\rangle + 0.097\|t_2e^2\rangle$	$0.902\|t_2^2e\rangle + 0.098\|t_2e^2\rangle$
Relative Energy (eV)	2.593	2.620
Relative Intensity	1.097	1.086

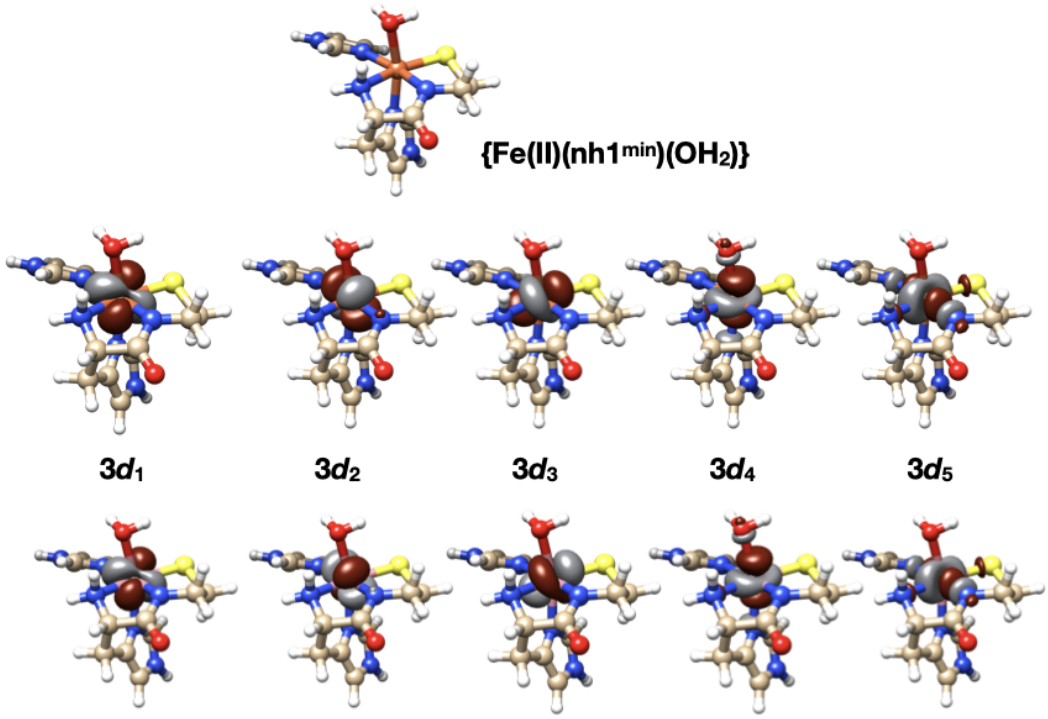

Figure S12. Top: Ball and stick figure of the minimized computational model of {Fe(II)(nh1)(OH_2)} used in the AILFT calculation. Middle: Isosurface plots (0.03 a.u.) of the MOs corresponding to the purified Fe(3d) orbitals outlined in Table SX. Bottom: Isosurface plots (0.03 a.u.) of the MOs corresponding to the purified Co(3d) orbitals outlined in Table SX

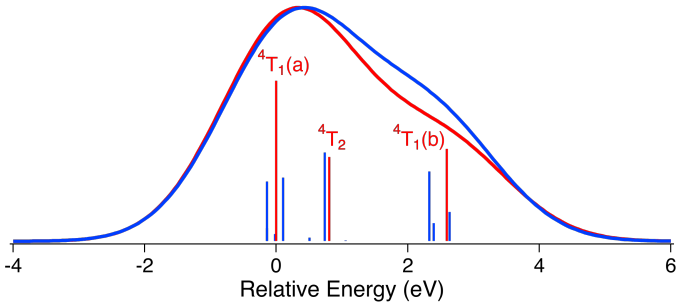

Figure S13. Simulated pre-edge features derived from 2-shell AILFT calculations of the minimized computational model of {Fe(II)(nh1)(OH_2)} (blue) vs solutions to the d^7 Tanabe-Sugano matrices using crystal-field input parameters derived from the 1-shell AILFT calculations of {Co(II)(nh1)(OH_2)} (red). The red and blue sticks correspond to the individual transitions. A 1.4 eV line width was applied to each transition.

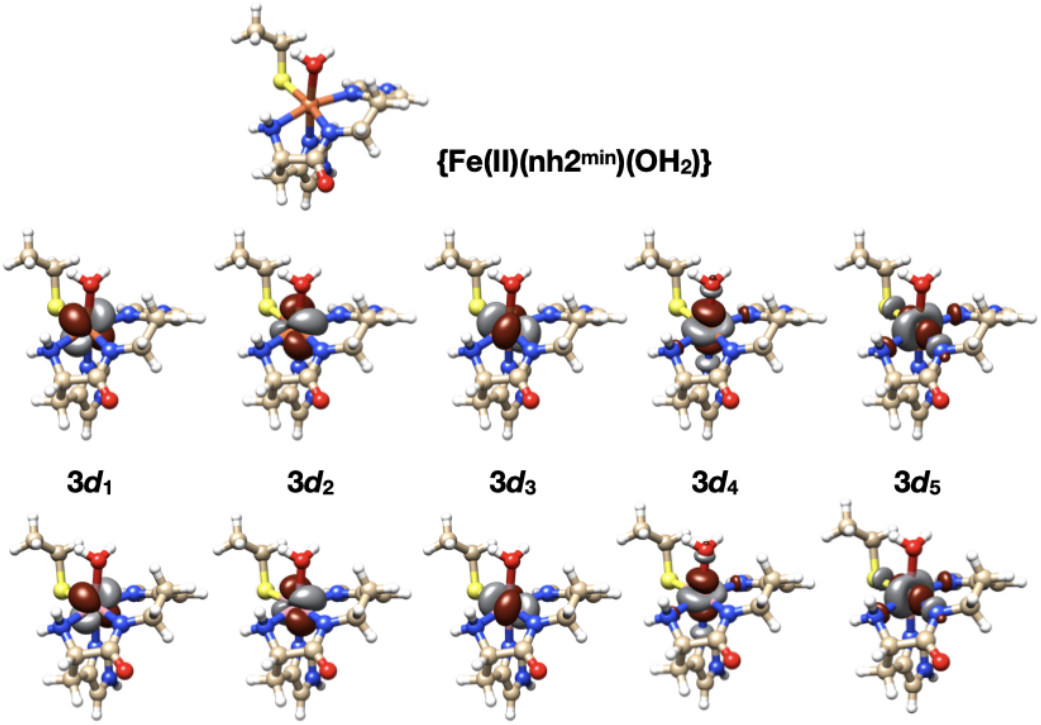

Figure S14. Top: Ball and stick figure of the minimized computational model of {Fe(II)(nh2)(OH_2)} used in the AILFT calculation. Middle: Isosurface plots (0.03 a.u.) of the MOs corresponding to the purified Fe(3d) orbitals outlined in Table SX. Bottom: Isosurface plots (0.03 a.u.) of the MOs corresponding to the purified Co(3d) orbitals outlined in Table SX

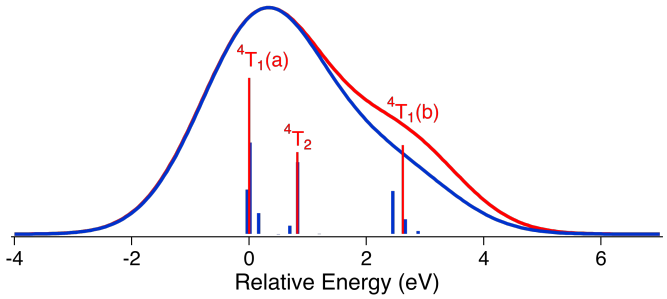

Figure S15. Simulated pre-edge features derived from 2-shell AILFT calculations of the minimized computational model of {Fe(II)(nh2)(OH_2)} (blue) vs solutions to the d^7 Tanabe-Sugano matrices using crystal-field input parameters derived from the 1-shell AILFT calculations of {Co(II)(nh2)(OH_2)} (red). The red and blue sticks correspond to the individual transitions. A 1.4 eV line width was applied to each transition.

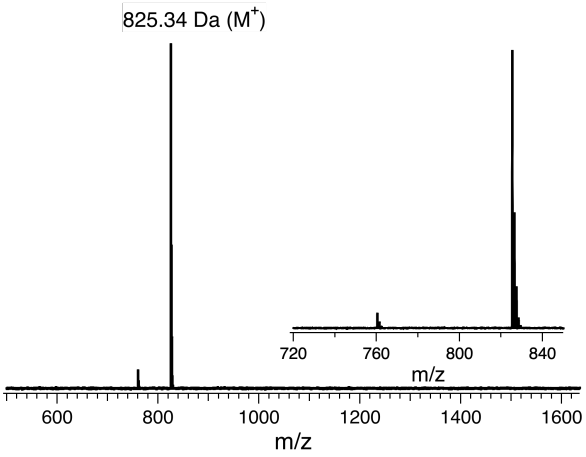

Figure S16. ESI-MS (positive ion mode) of peak 1 from the HPLC chromatogram in manuscript Fig. 5 obtained following injection of $^{16}O_2$(g) into solutions of {Fe(II)(nh1)(OH_2)} and subsequent filtration. The inset is zoomed in on the M^{+1} peak ($M+H^+$ calc: 825.35484 amu; found: 825.34 amu).

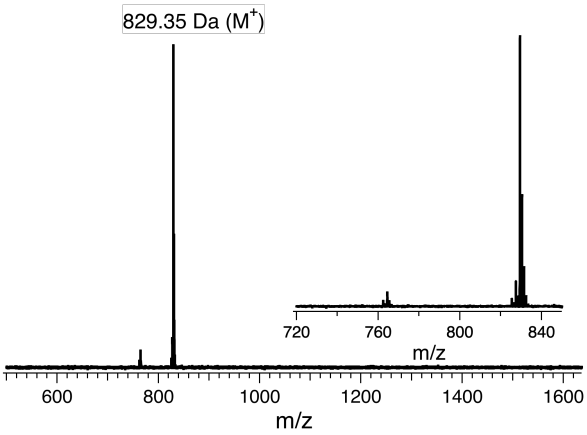

Figure S17. ESI-MS (positive ion mode) of peak 1 from the HPLC chromatogram in manuscript Fig. 5 obtained following injection of $^{18}O_2$(g) into solutions of {Fe(II)(nh1)(OH_2)} and subsequent filtration. The inset is zoomed in on the M^{+1} peak ($M+H^+$ calc: 829.35689 amu; found: 829.35 amu).

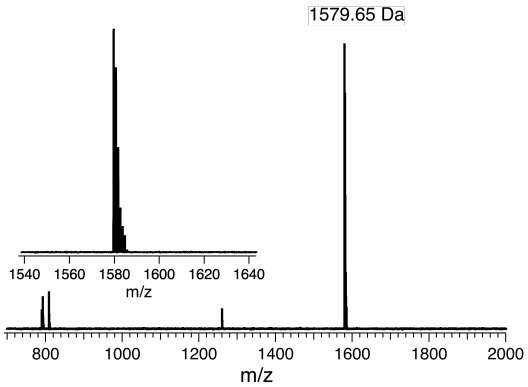

Figure S18. ESI-MS (positive ion mode) of peak 2 from the HPLC chromatogram in manuscript Fig. 5 obtained following injection of $^{16}O_2$(g) into solutions of {Fe(II)(nh1)(OH_2)} and subsequent filtration. The inset is zoomed in on the M^{+1} peak ($M+H^+$ calc: 1579.65344 amu; found: 1579.65 amu). Also present at $\sim$ 800 amu are the peaks resulting from cleavage of the S-S bond and the M^{+2} peak.

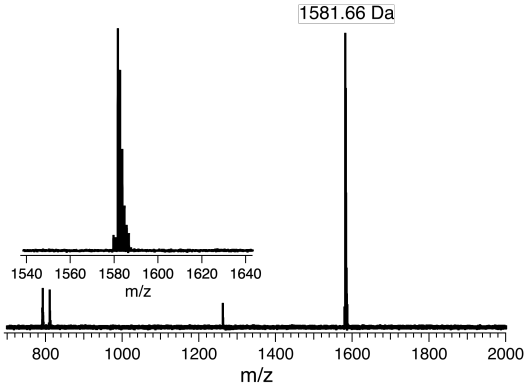

Figure S19. ESI-MS (positive ion mode) of peak 2 from the HPLC chromatogram in manuscript Fig. 5 obtained following injection of $^{18}O_2$(g) into solutions of {Fe(II)(nh1)(OH_2)} and subsequent filtration. The inset is zoomed in on the M^{+1} peak ($M+H^+$ calc: 1581.65769 amu; found: 1581.66 amu).Also present at $\sim$ 800 amu are the peaks resulting from cleavage of the S-S bond and the M^{+2} peak.

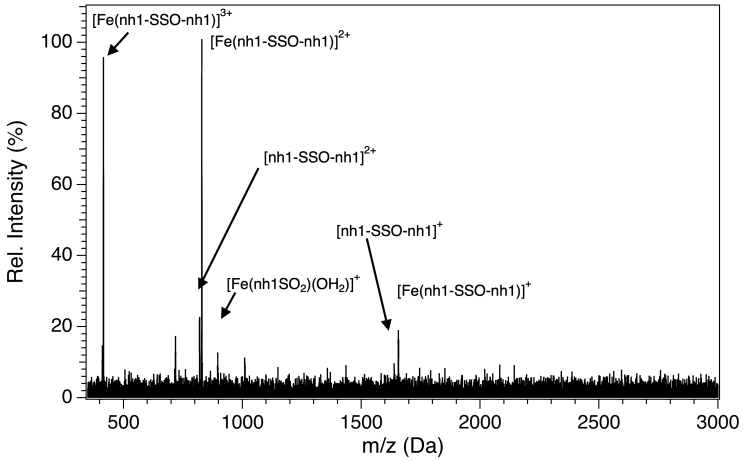

Figure S20. MALDI-TOF-MS (positive ion mode) of the solid generated in the reaction of {Fe(II)(nh1)(OH_2)} with O_2.

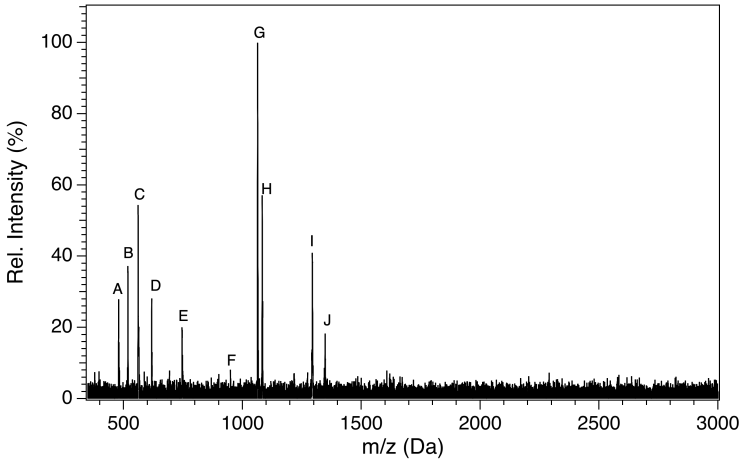

Figure S21. MALDI-TOF-MS (positive ion mode) of the solid generated in the reaction of {Fe(II)(nh1)(OH_2)} with O_2. Identified peaks from peptide cleavage or disulphide bond formation include A: HHDA, B: DLPCA, C: PCAPCA, D: HHDLP, E: HHDLPXA (X=C with loss of SH group), F: [Fe(HHDLPCCA)], G: [Fe(DLPCA)$_2$], H: [Fe(DLPCA)$_2$(OH_2)] I :[Fe(HHDLP)$_2$], J: HHDLPCADLPCA. All peptide with two Cys residues are likely the result of disulphide bond formation.

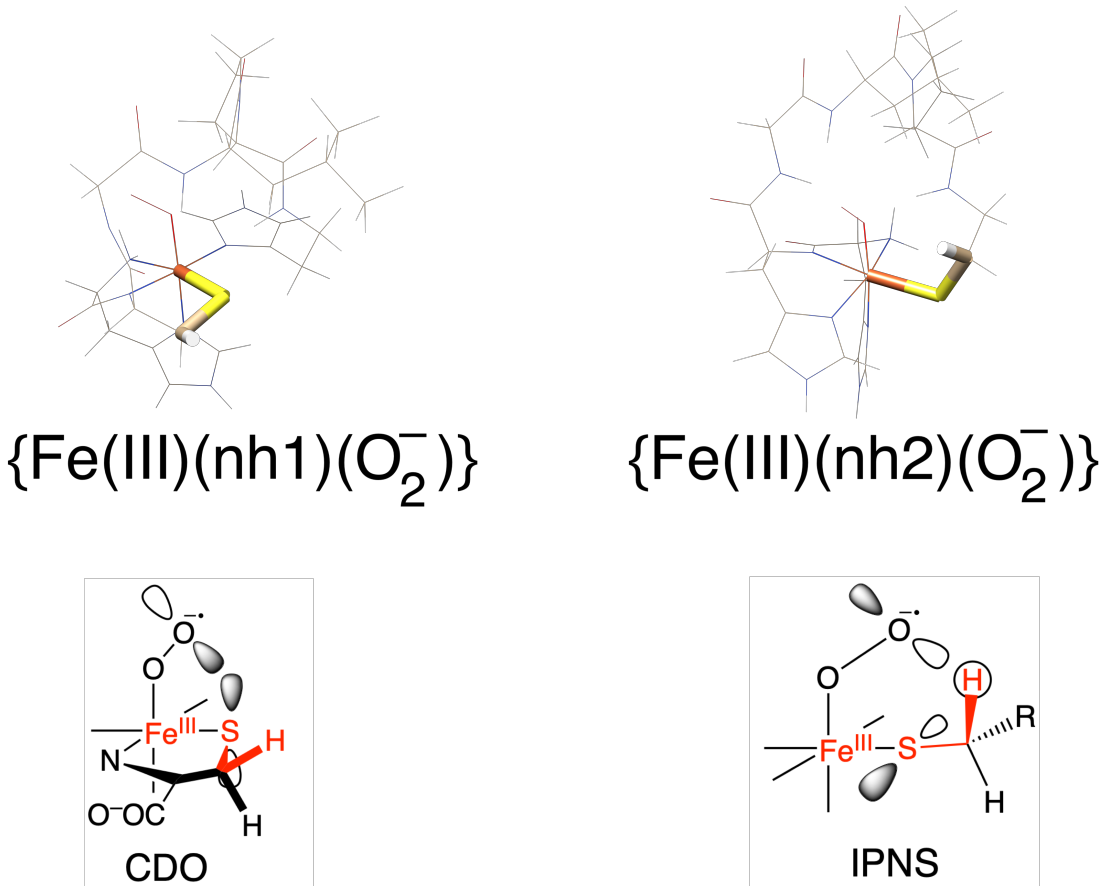

Figure S22. Top: wire representations of the minimized structures of {Fe(III)(nh1)(O_2^-)}. and {Fe(III)(nh1)(O_2^-)}. The highlighted Fe-S-C-H bonds depict the key elements comprising the dihedral angle, imposed by the manner in-which the peptide wraps around the Fe-centre, that orients the S(3p$_p i$) orbital in line or orthogonal to the superoxo moiety. Bottom: representations of the Fe(III)-O_2^- substrate bound forms of CDO vs IPNS with the highlighted Fe-S-C-H bonds that define the dihedral that orients the S(3p$_p i$) orbital in line or orthogonal to the superoxo moiety.

Table S6. Cartesian coordinates for the geometry optimized structure of {Fe(II)(nh1)(OH_2)}.

Fe	3.47104	27.72898	5.70441
O	2.54946	26.91513	7.68993
H	1.99918	26.11218	7.63921
H	1.98517	27.56697	8.14189
N	3.77277	25.50083	5.52671
C	5.198	25.36012	5.16587
C	6.06586	26.35024	5.96218
O	7.31376	26.16887	5.96573
C	5.36714	25.60486	3.65195
C	5.23751	27.03043	3.21028
N	4.31762	27.93349	3.73892
C	5.97249	27.67641	2.23954
C	4.4988	29.09008	3.09974
N	5.48591	28.96722	2.18302
N	5.3761	27.35378	6.51607
C	6.13293	28.4382	7.11988
C	5.96176	28.55414	8.63514
O	6.72381	29.25914	9.32217
C	5.67632	29.77111	6.48858
S	3.84028	29.9178	6.52457
N	4.89702	27.90352	9.15203
C	4.49719	28.04508	10.53076
C	3.79829	29.35435	10.91697
O	3.57391	29.5841	12.1174
N	3.43599	30.19753	9.92580

C	2.80993	31.48389	10.23181
C	1.42187	31.37261	10.90321
O	1.20487	32.01129	11.94959
C	2.78963	32.36062	8.97226
C	2.09443	33.71867	9.12814
C	2.81615	34.62924	10.12817
C	1.98499	34.3891	7.75401
N	0.45227	30.60359	10.35218
C	0.50168	29.84257	9.106780
C	0.08503	30.68243	7.88766
O	-0.72777	31.6175	7.96375
C	-0.52378	28.71708	9.36028
C	-1.60776	29.41918	10.19097
C	-0.82745	30.41057	11.06604
N	0.63508	30.26439	6.7318
C	0.334	30.85936	5.43634
C	0.989	30.03554	4.31823
C	0.611	28.59101	4.38409
H	5.56894	24.34407	5.3794
H	4.62954	24.97316	3.12654
H	6.35828	25.24363	3.34787
H	6.77933	27.33603	1.60099
H	3.97076	30.01586	3.29689
H	5.82089	29.70469	1.56876
H	7.21314	28.30913	6.93766
H	6.015	29.79839	5.44251
H	6.12563	30.61798	7.02553

H	4.29183	27.38358	8.51084
H	3.64518	29.97615	8.93507
H	3.41471	31.96973	11.01063
H	2.32106	31.80092	8.150700
H	3.83607	32.51935	8.661910
H	1.06984	33.54007	9.498390
H	3.85159	34.81514	9.79989
H	2.85154	34.18548	11.13268
H	2.3072	35.60116	10.20724
H	2.98616	34.57064	7.33116
H	1.46761	35.35701	7.82586
H	1.42986	33.75419	7.04751
H	1.51257	29.45147	8.94589
H	-0.0365	27.92369	9.94614
H	-0.8992	28.27859	8.42727
H	-2.19264	28.71546	10.79554
H	-2.29758	29.95895	9.52929
H	-1.34672	31.37035	11.18913
H	-0.61422	30.0107	12.06876
H	1.36653	29.55062	6.76218
H	2.08055	30.12566	4.41311
H	0.69389	30.46828	3.35282
H	-0.757934	30.88886	5.3053
H	0.7028	31.89761	5.40243
H	5.36991	27.9578	11.1933
H	3.80688	27.22747	10.78028
C	-0.55999	27.99014	3.97376

N	-0.47038	26.67054	4.36336
C	0.72002	26.48863	4.98119
N	1.40682	27.63315	5.01448
H	1.0373	25.53499	5.38576
H	-1.42954	28.38098	3.45817
H	-1.17082	25.95086	4.20456
H	3.19985	24.96764	4.86642
H	3.61203	25.08788	6.44865

Table S7. Cartesian coordinates for the geometry optimized structure of {Fe(II)(nh2)(OH_2)}.

Fe	3.660312962	28.13155086	4.88099199
O	3.505405718	29.99376268	6.488194338
H	2.531580546	30.15342597	6.510025762
H	3.862468956	30.75426887	5.992060623
N	2.863536914	26.55876646	6.246852457
C	3.926428673	25.53710076	6.352684576
C	5.301869156	26.22032234	6.444639161
O	6.271858017	25.54795805	6.885217368
C	3.848630455	24.5548088	5.176313912
C	4.197838568	25.1211191	3.833258083
N	4.021707562	26.45622154	3.481684884
C	4.687045001	24.43561557	2.739900376
C	4.38453406	26.5635901	2.203487462
N	4.788944471	25.36175654	1.72331953
N	5.315503582	27.50846832	6.070379058
C	6.572690576	28.1928785	6.324197044
C	6.797127844	28.41075972	7.836453383
O	7.918112428	28.63900735	8.315093825
C	6.639710424	29.60768619	5.697700542
N	5.64674172	28.41984696	8.554772131
C	5.585686038	28.58433021	9.985186576
C	4.566268651	29.59621611	10.5009844
O	4.4127703	29.72604372	11.72574936
N	3.858654663	30.30828218	9.59358099
C	2.908494521	31.33056767	10.02954433

C	1.685078276	30.76852819	10.79311163
O	1.385101114	31.2717417	11.89153893
C	2.528957885	32.23210314	8.847873725
C	1.562502986	33.37630278	9.180888411
C	2.161543924	34.37735532	10.17476533
C	1.14777218	34.07495196	7.881000895
N	0.958673846	29.7447615	10.28284088
C	1.051323461	29.12803345	8.962425972
C	0.280156906	29.94914378	7.906814304
O	-0.549218472	30.81126953	8.210089327
C	0.389533592	27.75326768	9.186823571
C	-0.742027856	28.08058162	10.17117893
C	-0.146526537	29.16696402	11.0779567
N	0.627235986	29.66238798	6.618483467
C	-0.031071361	30.26332799	5.460638454
C	0.916920138	30.27176756	4.262018292
S	1.567828842	28.59689807	3.849330911
H	1.985988253	26.14223471	5.926018383
H	3.815575367	24.94707028	7.277330924
H	2.82692221	24.13674446	5.155170643
H	4.520679304	23.71156286	5.386927952
H	4.957177479	23.39494975	2.60184715
H	4.379822764	27.46973248	1.610292393
H	5.118204745	25.1801458	0.779193002
H	7.43136433	27.59954443	5.96785462
H	4.818562828	28.1245081	8.035040247
H	4.026219632	30.18503981	8.589616831

H	3.410196955	31.9355654	10.79742614
H	2.083498265	31.62436641	8.049431465
H	3.462992561	32.65039023	8.436209277
H	0.65741218	32.93433257	9.630839205
H	3.087769258	34.81609253	9.76967051
H	2.399703223	33.9072684	11.13888645
H	1.455721888	35.19849055	10.36773482
H	2.025546042	34.51453198	7.380528843
H	0.431148625	34.8850355	8.079983838
H	0.67949057	33.36488003	7.18328085
H	2.097313068	29.02210274	8.651890834
H	1.129949258	27.0826317	9.645115079
H	0.041158576	27.29672372	8.251879351
H	-1.068093205	27.20379732	10.74331875
H	-1.611911876	28.47440693	9.628015257
H	-0.872933174	29.94618103	11.34395722
H	0.266218186	28.75579445	12.01139549
H	1.082842317	28.76682127	6.408647113
H	1.758576523	30.95405823	4.451992691
H	0.369673558	30.65845184	3.391386398
H	2.68169048	26.95756563	7.170638488
H	-0.948892009	29.7035905	5.215097963
H	-0.318169863	31.28766003	5.735685853
H	6.578687423	28.90374111	10.33278169
H	5.355206432	27.63035709	10.48719021
C	6.248906377	29.73350195	4.264992234
N	4.956309008	29.46459516	3.823960621

C	6.97491652	30.24519541	3.209869371
N	6.106670165	30.2971813	2.137441773
C	4.901991772	29.82464427	2.541632208
H	4.028419988	29.75953134	1.901809241
H	6.326844928	30.64236048	1.20711951
H	7.666228043	29.97815448	5.820189126
H	5.994733696	30.27402613	6.291925598
H	8.000130614	30.58989878	3.138582501

Table S8. Cartesian coordinates for the geometry optimized structure of the AILFT minimized model {Fe/Co(II)(nh1)(OH_2)}.

Fe/Co	3.42088	27.67359	5.82815
O	2.50212	26.932	7.71875
H	1.52737	26.98171	7.67631
H	2.74978	27.66634	8.31716
N	3.77001	25.43558	5.60741
C	5.19087	25.32338	5.21747
C	6.06119	26.33166	5.98772
O	7.31245	26.1721	5.95267
H	1.00831	25.5278	5.21833
C	5.17817	26.99128	3.26948
N	4.26683	27.88208	3.823
C	5.89759	27.64403	2.29302
C	4.43793	29.04074	3.18996
N	5.40929	28.93237	2.25558
N	5.37249	27.32195	6.56356
C	6.12664	28.41707	7.14936
H	5.94771	28.46576	8.24014
H	-1.13308	25.98357	3.92961
C	5.65205	29.7411	6.51379
S	3.81616	29.88866	6.58787
H	-1.36633	28.43694	3.28189
N	-0.4465	26.69689	4.16192
H	0.92806	29.65485	4.30306
H	5.5884	24.31411	5.4259
C	0.61176	28.61814	4.34407

C	0.7067	26.49807	4.84048
N	1.37841	27.64132	4.9734
C	-0.52577	28.03156	3.83393
H	3.64201	25.10862	6.56891
H	6.69552	27.31054	1.63896
H	3.90594	29.96201	3.40179
H	5.73223	29.67672	1.64308
H	7.21121	28.28568	6.99002
H	5.97067	29.77631	5.45971
H	3.20704	24.82069	5.01164
H	6.11029	30.59767	7.03319
C	5.32212	25.56475	3.70008
H	4.57549	24.92944	3.19007
H	6.30659	25.20506	3.37037

Table S9. Cartesian coordinates for the geometry optimized structure of the AILFT minimized model {Fe/Co(II)(nh2)(OH_2)}.

Fe/Co	3.65822	28.19636	4.95089
O	3.46253	29.90206	6.38009
H	2.57804	30.04192	6.76754
H	3.66713	30.74082	5.92544
N	2.88224	26.58045	6.28215
C	3.94579	25.55657	6.36433
C	5.3232	26.2349	6.45481
O	6.29577	25.55201	6.87463
H	7.67144	30.01884	5.89046
C	4.21434	25.17913	3.84296
N	4.02476	26.51393	3.51044
C	4.72062	24.51097	2.74823
C	4.39611	26.63669	2.2385
N	4.81975	25.44845	1.74455
N	5.33573	27.52866	6.10444
C	6.59089	28.21131	6.36735
H	6.76996	28.29611	7.4559
H	1.99991	26.16689	5.96956
C	6.64873	29.63435	5.75906
H	3.84051	24.94089	7.27433
H	4.0733	29.82379	1.9467
N	4.97858	29.51248	3.87709
C	7.00917	30.27122	3.27656
C	6.26859	29.7684	4.32422
H	5.9913	30.29135	6.35159

H	8.03884	30.60538	3.213
H	5.00251	23.47435	2.59992
H	4.38485	27.54675	1.65094
H	5.15935	25.28321	0.80088
H	7.44291	27.62693	5.96877
H	6.38084	30.67532	1.2699
H	0.31786	30.6284	3.41221
N	6.15164	30.33243	2.19891
H	-0.48106	31.21067	5.72279
H	-0.9291	29.53673	5.30257
H	2.7095	26.97841	7.20887
C	4.94075	29.87362	2.59684
H	1.68751	30.95516	4.47813
H	0.43192	29.83606	6.39599
C	-0.07923	30.20874	5.49499
C	0.86201	30.2522	4.29232
S	1.5612	28.60272	3.85943
C	3.84412	24.59846	5.15627
H	2.80974	24.20978	5.12604
H	4.48583	23.72752	5.35384

Table S10. Cartesian coordinates for the geometry optimized structure of low-spin {Fe(III)(nh1)(O_2^-)} possessing an $s = \frac{1}{2}$ Fe(III) center antiferromagnetically coupled to the $s = \frac{1}{2}$ O_2^- ($J = -934.96$ cm^{-1}).

O	2.698875013	27.70578123	7.345827735
O	2.920869304	26.70587768	8.208206245
Fe	3.526734311	27.77446678	5.762623927
N	3.510434048	25.75925633	5.809860648
C	4.890036002	25.27111654	5.610155664
C	5.85232245	26.25439531	6.291601851
O	7.029478055	25.93777595	6.549741658
C	5.192462921	25.1609067	4.112279254
C	4.943248205	26.43455672	3.351743229
N	4.244049192	27.52784971	3.862196953
C	5.293248261	26.72053664	2.040290904
C	4.173164218	28.4431148	2.886551979
N	4.795199233	27.98097052	1.776463655
N	5.273009715	27.46118097	6.495696324
C	6.085265173	28.56073337	6.992193867
C	5.780384781	28.97791424	8.443530504
O	6.192049835	30.07222666	8.888086257
C	5.908086644	29.74616467	6.052323043
S	4.110263561	29.96607853	5.730757487
N	5.110274622	28.08408777	9.199078007
C	4.855345335	28.2872417	10.6136363
C	3.694369372	29.23503891	10.97569465
O	2.894110692	28.9547285	11.87832941
N	3.655273778	30.38486455	10.24961891

C	2.755409866	31.50168512	10.53838352
C	1.338021841	31.07516377	10.989374
O	0.890926833	31.50866162	12.06659659
C	2.765951133	32.46284835	9.332258829
C	1.68727174	33.56035011	9.339358657
C	1.782796822	34.47043565	10.57346298
C	1.764785373	34.36838762	8.035991348
N	0.578307314	30.27262078	10.19662601
C	0.898839478	29.73594893	8.873072291
C	0.381620423	30.65425064	7.749543384
O	-0.714850643	31.23384548	7.814912698
C	0.114962499	28.40410084	8.851848935
C	-1.158527063	28.73558503	9.647883467
C	-0.68669804	29.73011882	10.72417095
N	1.204423426	30.70651777	6.673993411
C	0.853545711	31.32057943	5.405977042
C	1.291331646	30.44390732	4.209868569
C	0.865301586	29.01692389	4.369287438
H	5.027870397	24.2705579	6.070467784
H	4.569274327	24.34393216	3.685620856
H	6.247578056	24.84476861	3.987706035
H	5.840710963	26.13733669	1.293695681
H	3.715934004	29.43250616	2.966231567
H	4.892602125	28.49323508	0.895244581
H	7.150272701	28.22783971	7.003516292
H	6.418824023	29.55193018	5.087696184
H	6.312650215	30.67276708	6.50247023

H	4.568533125	27.33402937	8.725561486
H	4.484411032	30.57774713	9.659388689
H	3.127611797	32.04211513	11.43525304
H	2.672872012	31.86975717	8.401137998
H	3.771862654	32.93773337	9.289676395
H	0.69515288	33.05495067	9.35741271
H	2.781155079	34.95594905	10.62932854
H	1.621197208	33.90012996	11.50954283
H	1.018845007	35.27413056	10.53060609
H	2.739002666	34.89688582	7.953991867
H	0.96116686	35.13162466	7.988841911
H	1.663701743	33.70963444	7.149197859
H	1.984617854	29.56733366	8.761819869
H	0.734749675	27.63109889	9.348191234
H	-0.082344594	28.05551694	7.820074155
H	-1.632079421	27.83865135	10.09208334
H	-1.897038328	29.22479666	8.984276133
H	-1.416950057	30.54324846	10.91287817
H	-0.480873007	29.24130556	11.70093157
H	2.129460514	30.25414113	6.745526097
H	2.391139278	30.50897048	4.099912892
H	0.843642585	30.86696058	3.288614969
H	-0.245301166	31.46492271	5.412979685
H	1.317574037	32.32764403	5.3081744
H	5.773046682	28.69851789	11.08785176
H	4.628942864	27.31291903	11.0832109
C	-0.402856048	28.52005942	4.097203099

N	-0.419694265	27.22340866	4.560187436
C	0.794605504	26.94459474	5.091380082
N	1.610427559	28.00523515	4.987667823
H	1.017808891	25.98230163	5.559219105
H	-1.27498501	28.99210858	3.634669001
H	-1.20903904	26.57259619	4.516432177
H	2.858713446	25.24384612	5.199697208
H	3.225458508	25.63193531	6.814091678

Table S11. Cartesian coordinates for the geometry optimized structure of intermediate-spin {Fe(III)(nh1)(O_2^-)} possessing an $s = \frac{3}{2}$ Fe(III) center antiferromagnetically coupled to the $s = \frac{1}{2}$ O_2^- ($J = -893.67$ cm^{-1})

O	2.698875013	27.70578123	7.345827735
O	2.920869304	26.70587768	8.208206245
Fe	3.526734311	27.77446678	5.762623927
N	3.510434048	25.75925633	5.809860648
C	4.890036002	25.27111654	5.610155664
C	5.85232245	26.25439531	6.291601851
O	7.029478055	25.93777595	6.549741658
C	5.192462921	25.1609067	4.112279254
C	4.943248205	26.43455672	3.351743229
N	4.244049192	27.52784971	3.862196953
C	5.293248261	26.72053664	2.040290904
C	4.173164218	28.4431148	2.886551979
N	4.795199233	27.98097052	1.776463655
N	5.273009715	27.46118097	6.495696324
C	6.085265173	28.56073337	6.992193867
C	5.780384781	28.97791424	8.443530504
O	6.192049835	30.07222666	8.888086257
C	5.908086644	29.74616467	6.052323043
S	4.110263561	29.96607853	5.730757487
N	5.110274622	28.08408777	9.199078007
C	4.855345335	28.2872417	10.6136363
C	3.694369372	29.23503891	10.97569465
O	2.894110692	28.9547285	11.87832941
N	3.655273778	30.38486455	10.24961891

C	2.755409866	31.50168512	10.53838352
C	1.338021841	31.07516377	10.989374
O	0.890926833	31.50866162	12.06659659
C	2.765951133	32.46284835	9.332258829
C	1.68727174	33.56035011	9.339358657
C	1.782796822	34.47043565	10.57346298
C	1.764785373	34.36838762	8.035991348
N	0.578307314	30.27262078	10.19662601
C	0.898839478	29.73594893	8.873072291
C	0.381620423	30.65425064	7.749543384
O	-0.714850643	31.23384548	7.814912698
C	0.114962499	28.40410084	8.851848935
C	-1.158527063	28.73558503	9.647883467
C	-0.68669804	29.73011882	10.72417095
N	1.204423426	30.70651777	6.673993411
C	0.853545711	31.32057943	5.405977042
C	1.291331646	30.44390732	4.209868569
C	0.865301586	29.01692389	4.369287438
H	5.027870397	24.2705579	6.070467784
H	4.569274327	24.34393216	3.685620856
H	6.247578056	24.84476861	3.987706035
H	5.840710963	26.13733669	1.293695681
H	3.715934004	29.43250616	2.966231567
H	4.892602125	28.49323508	0.895244581
H	7.150272701	28.22783971	7.003516292
H	6.418824023	29.55193018	5.087696184
H	6.312650215	30.67276708	6.50247023

H	4.568533125	27.33402937	8.725561486
H	4.484411032	30.57774713	9.659388689
H	3.127611797	32.04211513	11.43525304
H	2.672872012	31.86975717	8.401137998
H	3.771862654	32.93773337	9.289676395
H	0.69515288	33.05495067	9.35741271
H	2.781155079	34.95594905	10.62932854
H	1.621197208	33.90012996	11.50954283
H	1.018845007	35.27413056	10.53060609
H	2.739002666	34.89688582	7.953991867
H	0.96116686	35.13162466	7.988841911
H	1.663701743	33.70963444	7.149197859
H	1.984617854	29.56733366	8.761819869
H	0.734749675	27.63109889	9.348191234
H	-0.082344594	28.05551694	7.820074155
H	-1.632079421	27.83865135	10.09208334
H	-1.897038328	29.22479666	8.984276133
H	-1.416950057	30.54324846	10.91287817
H	-0.480873007	29.24130556	11.70093157
H	2.129460514	30.25414113	6.745526097
H	2.391139278	30.50897048	4.099912892
H	0.843642585	30.86696058	3.288614969
H	-0.245301166	31.46492271	5.412979685
H	1.317574037	32.32764403	5.3081744
H	5.773046682	28.69851789	11.08785176
H	4.628942864	27.31291903	11.0832109
C	-0.402856048	28.52005942	4.097203099

N	-0.419694265	27.22340866	4.560187436
C	0.794605504	26.94459474	5.091380082
N	1.610427559	28.00523515	4.987667823
H	1.017808891	25.98230163	5.559219105
H	-1.27498501	28.99210858	3.634669001
H	-1.20903904	26.57259619	4.516432177
H	2.858713446	25.24384612	5.199697208
H	3.225458508	25.63193531	6.814091678

Table S12. Cartesian coordinates for the geometry optimized structure of high-spin {Fe(III)(nh1)(O_2^-)} possessing an $s = \frac{5}{2}$ Fe(III) center antiferromagnetically coupled to the $s = \frac{1}{2}$ O_2^- ($J = -220.70$ cm^{-1})

O	2.803405	27.77072	7.412058
O	2.952582	26.695307	8.214964
Fe	3.533011	27.80946	5.737252
N	3.47128	25.795692	5.816467
C	4.840432	25.279737	5.620029
C	5.824032	26.251149	6.289286
O	6.990424	25.91292	6.565628
C	5.140849	25.147845	4.122836
C	4.948451	26.427489	3.356333
N	4.27602	27.543003	3.853959
C	5.339262	26.706523	2.055114
C	4.259495	28.464687	2.881121
N	4.891094	27.983845	1.784393
N	5.275772	27.477547	6.46042
C	6.090555	28.56803	6.967787
C	5.790816	28.974442	8.4256030
O	6.193911	30.073463	8.8670970
C	5.911193	29.763519	6.038534
S	4.110805	29.981831	5.72193
N	5.14043	28.0718	9.187987
C	4.884378	28.289503	10.600625
C	3.704548	29.21897	10.951885
O	2.897736	28.92376	11.843985
N	3.657358	30.37283	10.232086

C	2.74985	31.481967	10.528989
C	1.332154	31.046839	10.971603
O	0.883044	31.463431	12.054619
C	2.759289	32.456339	9.333568
C	1.672149	33.545479	9.347546
C	1.75902	34.446281	10.589124
C	1.744145	34.364065	8.050526
N	0.572942	30.258623	10.163981
C	0.901136	29.738446	8.83619
C	0.380583	30.661181	7.717441
O	-0.725332	31.222751	7.775147
C	0.128996	28.400344	8.799363
C	-1.150224	28.71341	9.594118
C	-0.691333	29.703781	10.680353
N	1.21725	30.737448	6.65333
C	0.873625	31.338526	5.377288
C	1.283932	30.430988	4.192139
C	0.8464	29.014133	4.398686
H	4.960025	24.281858	6.091201
H	4.484351	24.355371	3.699762
H	6.182201	24.788077	4.001175
H	5.884061	26.107245	1.319383
H	3.832727	29.468444	2.954526
H	5.025991	28.494652	0.907217
H	7.155297	28.234427	6.972539
H	6.419526	29.57719	5.071584
H	6.312504	30.688422	6.494537

H	4.574387	27.327015	8.729285
H	4.486795	30.575474	9.6457
H	3.116858	32.014311	11.432842
H	2.67419	31.872612	8.395971
H	3.761642	32.939353	9.300548
H	0.683787	33.032567	9.360443
H	2.752911	34.940316	10.649482
H	1.602277	33.86676	11.520374
H	0.987783	35.243309	10.552791
H	2.715477	34.898267	7.971293
H	0.936538	35.123487	8.010477
H	1.644859	33.711376	7.159146
H	1.988376	29.577533	8.72611
H	0.754234	27.627888	9.289636
H	-0.063402	28.059048	7.763952
H	-1.615822	27.80824	10.030046
H	-1.891541	29.200183	8.93196
H	-1.428816	30.510127	10.870516
H	-0.487834	29.209712	11.654851
H	2.143735	30.291195	6.734378
H	2.381894	30.4795	4.06085
H	0.824452	30.836339	3.268743
H	-0.221815	31.505988	5.388689
H	1.359642	32.33276	5.26076
H	5.794578	28.72446	11.067673
H	4.675719	27.317285	11.082849
C	-0.437764	28.528232	4.191779

N	-0.455077	27.248277	4.699803
C	0.773649	26.967499	5.193638
N	1.60073	28.011106	5.020934
H	0.998613	26.01995	5.689255
H	-1.320854	28.997929	3.748119
H	-1.255156	26.609136	4.708795
H	2.805327	25.283528	5.219548
H	3.18971	25.705917	6.834215

Table S13. Cartesian coordinates for the geometry optimized structure of low-spin {Fe(III)(nh2)(O_2^-)} possessing an $s = \frac{1}{2}$ Fe(III) center antiferromagnetically coupled to the $s = \frac{1}{2}$ O_2^- ($J = -551.22$ cm^{-1}).

O	3.827459631	29.19551706	6.516255547
O	4.224440334	30.46517405	6.623926141
Fe	4.151473918	28.12828212	5.068722944
N	3.288289835	26.66104121	6.116116883
C	4.264954667	25.55266695	6.24531834
C	5.660923999	26.17026634	6.431850079
O	6.571050873	25.53759709	7.002053157
C	4.20163686	24.64175648	5.019276235
C	4.509618794	25.35650994	3.736583019
N	4.449300202	26.73948264	3.592707209
C	4.853179155	24.79936634	2.515603563
C	4.743371859	27.00381814	2.313853305
N	4.989387738	25.85569062	1.641867076
N	5.752313907	27.44018358	5.959323683
C	6.963637019	28.15095896	6.340176853
C	7.088694289	28.28038412	7.880657949
O	8.186211966	28.33077561	8.447802344
C	7.034770143	29.60361883	5.810129861
N	5.891928376	28.45124366	8.516156821
C	5.774824666	28.65001083	9.940218299
C	4.861609511	29.784358	10.42041381
O	4.686298237	29.9297459	11.64106547
N	4.250602954	30.56697619	9.494193538
C	3.345032367	31.63298946	9.920191035

C	2.162100009	31.14678143	10.79525447
O	1.904034337	31.73975251	11.85784597
C	2.892693217	32.44257158	8.690164577
C	1.794347558	33.48989303	8.935985307
C	2.196519887	34.53095101	9.990947808
C	1.420824054	34.15604852	7.60342641
N	1.40191781	30.09175824	10.38973174
C	1.452513091	29.36180585	9.123130307
C	0.655842126	30.09047688	8.015217871
O	-0.30288233	30.84186415	8.255206245
C	0.783473335	28.01818491	9.486756324
C	-0.32089103	28.44883397	10.46663975
C	0.322701649	29.59551762	11.26544629
N	1.094340905	29.77938768	6.774097587
C	0.606003015	30.36556692	5.536645795
C	1.703002708	30.33287109	4.467621823
S	2.203882034	28.61646326	4.005414327
H	2.400506418	26.34190969	5.699268941
H	4.049834782	24.94373027	7.146758445
H	3.189764877	24.18153328	4.970417385
H	4.91668552	23.80778207	5.163873331
H	5.000254537	23.75899099	2.21114802
H	4.791830858	27.98966578	1.84632213
H	5.239193818	25.79321747	0.651108833
H	7.859612198	27.58369142	6.008764548
H	5.040976187	28.35942975	7.947354965
H	4.405338291	30.46272476	8.468025347

H	3.891008371	32.29615756	10.62256206
H	2.563365137	31.7383458	7.90019906
H	3.794280678	32.9461992	8.275465191
H	0.892501146	32.94857683	9.299422689
H	3.13309963	35.0518172	9.695291201
H	2.357877981	34.05691044	10.97904562
H	1.406594591	35.30160601	10.10915884
H	2.28437281	34.71713289	7.185305634
H	0.582644336	34.87160246	7.7311715
H	1.114760987	33.4010374	6.850115663
H	2.496132137	29.21770044	8.789716542
H	1.533174681	27.37227474	9.988876551
H	0.408619661	27.48099267	8.594196053
H	-0.664159318	27.62504343	11.1214296
H	-1.196142172	28.82704144	9.90268993
H	-0.388463995	30.41113535	11.50665593
H	0.764926032	29.25155819	12.22529636
H	1.973222312	29.24797146	6.704913965
H	2.601132789	30.88071352	4.823734142
H	1.332814246	30.83393885	3.550810337
H	3.042394007	27.02970169	7.048895641
H	-0.296917953	29.82600334	5.171414474
H	0.295604106	31.41475737	5.736092951
H	6.793467082	28.84008611	10.33595967
H	5.402982698	27.73481589	10.45296603
C	6.463871191	29.87954838	4.462185636
N	5.177719638	29.49445928	4.108078812

C	6.952475822	30.72262073	3.475634621
N	5.942451174	30.85025521	2.545817288
C	4.886615767	30.10486133	2.952413369
H	3.940353109	30.01288841	2.409330599
H	5.976385751	31.40925161	1.689161486

Table S14. Cartesian coordinates for the geometry optimized structure of intermediate-spin {Fe(III)(nh2)(O_2^-)} possessing an $s = \frac{3}{2}$ Fe(III) center antiferromagnetically coupled to the $s = \frac{1}{2}$ O_2^- ($J = -1379.70$ cm^{-1})

O	3.67227454	29.03779346518114	6.426268797
O	4.041682209	30.3227718505028	6.63583812
Fe	4.167348056	28.02459582794835	4.941917127
N	3.444306846	26.43053657504085	5.94809987
C	4.523654915	25.41653024690968	6.072528836
C	5.841836812	26.16187395564539	6.315962897
O	6.801924047	25.58295923004404	6.871662985
C	4.565340517	24.5347682886538	4.82519774
C	4.801164279	25.29309712362543	3.553142763
N	4.616730595	26.66834588411721	3.422319667
C	5.174120223	24.77992359361261	2.330796178
C	4.866806897	26.96161210092443	2.142926576
N	5.20392794	25.84615924234353	1.462478526
N	5.806352903	27.45310146661868	5.924758291
C	6.951280328	28.26002959051254	6.342536375
C	7.047305634	28.41082687197969	7.882973998
O	8.141809739	28.56352639063874	8.444872446
C	6.941402234	29.71388902620701	5.802776737
N	5.850904307	28.46895146858024	8.523155608
C	5.713684405	28.66660457273134	9.950224843
C	4.769701016	29.77297448333377	10.439419650
O	4.681709234	29.95198503749855	11.666953981
N	4.052928732	30.48618589411539	9.540326952
C	3.193037013	31.58871219711143	9.985429185

C	1.948698298	31.17700223506877	10.815349185
O	1.730982019	31.79207205330808	11.877912792
C	2.831836083	32.49440945399179	8.791520663
C	2.111335371	33.80896186589245	9.146782065
C	2.989954600	34.75681431511241	9.975416960
C	1.644353846	34.50076216421745	7.857541189
N	1.093156758	30.20305124851417	10.40728642
C	1.155798452	29.34245751426923	9.217966555
C	0.397025623	29.93022573622723	8.004858446
O	-0.610262862	30.64788816897586	8.12903478
C	0.455837737	28.05192716620467	9.705547655
C	-0.642703524	28.576974899151	10.641615167
C	-0.002364378	29.79581568664257	11.3207867
N	0.898718676	29.52656446799761	6.818305266
C	0.36814961	29.92663431427217	5.519836542
C	1.473620238	29.99887551351542	4.462958988
S	2.177679021	28.37278622893903	3.963603286
H	2.608873276	26.02923290825352	5.510125475
H	4.340663825	24.77272093134772	6.945658537
H	3.61357159	23.97988949035336	4.762120957
H	5.353034405	23.77919306637268	4.957931506
H	5.407402121	23.76887898972199	2.017730608
H	4.821854665	27.93985293509683	1.683114831
H	5.442792886	25.81022679449428	0.474820456
H	7.882942888	27.7618840306663	6.030279698
H	5.018464383	28.28306520311742	7.961161107
H	4.164994394	30.35495718647781	8.515555394

H	3.771008398	32.17337805636222	10.715202700
H	2.218769827	31.92723851571287	8.074449376
H	3.772275955	32.73765287381197	8.268266694
H	1.212841293	33.56607254138046	9.740808479
H	3.901921812	35.02559846080136	9.417628162
H	3.296463054	34.31155904213767	10.932438657
H	2.448458697	35.68764434270542	10.201250816
H	2.504896133	34.75979259414137	7.219501359
H	1.1031974	35.43138485510699	8.084696337
H	0.974854291	33.85132110350027	7.274134288
H	2.197716622	29.14801718256972	8.940318751
H	1.186321743	27.44594456590661	10.261394299
H	0.070909101	27.44756997470466	8.874227788
H	-0.962245548	27.82570643561881	11.3748919337
H	-1.52254149	28.88320899866043	10.06056068338
H	-0.708400993	30.62448138505884	11.4686560619
H	0.432318988	29.55025532959599	12.3017108852
H	1.818805758	29.07033603218945	6.810441292
H	2.28968998	30.64982073520399	4.805252567
H	1.048272495	30.43448256493673	3.54746571
H	3.157651842	26.76193485470338	6.876474252
H	-0.421788646	29.22869032246162	5.194398686
H	-0.096511800	30.91939901086584	5.62617903
H	6.711126975	28.89124196020028	10.352682617
H	5.369396925	27.74172280129482	10.442896487
C	6.3912182	29.95414054849787	4.440970811
N	5.144627589	29.4897091324224	4.037545676

C	6.85471757	30.83228822471239	3.48505925
N	5.874000698	30.90782470526567	2.52209395
C	4.857475491	30.0936209640454	2.880152234
H	3.949198926	29.96114186865385	2.303553757
H	5.901546874	31.47882480487894	1.681465078
H	7.967945432	30.10058804296102	5.849641561
H	6.326557853	30.32525031891556	6.484008446
H	7.764899135	31.41827789792616	3.433641903

Table S15. Cartesian coordinates for the geometry optimized structure of high-spin {Fe(III)(nh2)(O_2^-)} possessing an $s = \frac{5}{2}$ Fe(III) center antiferromagnetically coupled to the $s = \frac{1}{2}$ O_2^- ($J = -108.71$ cm^{-1})

O	3.870329476	29.2079583	6.5032063
O	4.244784675	30.50257548	6.611166614
Fe	4.170231857	28.14559557	5.013990755
N	3.269559117	26.68623331	6.055328196
C	4.209061424	25.54638563	6.173439535
C	5.614690607	26.12648203	6.395341144
O	6.50032315	25.4686429	6.975883468
C	4.136247708	24.66262308	4.928404047
C	4.481818523	25.38705911	3.660434516
N	4.454573131	26.77262907	3.528779421
C	4.828431967	24.83468781	2.438211599
C	4.770014601	27.04256825	2.255759812
N	4.998876195	25.89569697	1.576295536
N	5.735938144	27.39936906	5.943311112
C	6.947122753	28.09025071	6.364022691
C	7.038721211	28.19628167	7.907260317
O	8.122595799	28.17619363	8.503979819
C	7.050089094	29.54885501	5.857367632
N	5.836546606	28.42574945	8.510125681
C	5.700308355	28.63840635	9.929854397
C	4.84129782	29.82135438	10.3896686
O	4.672731778	29.98906054	11.60928514
N	4.253701311	30.61088021	9.454619806
C	3.351647461	31.68159979	9.877211593

C	2.196720457	31.20312098	10.79311137
O	1.949013928	31.82542863	11.8412513
C	2.855433325	32.45241439	8.638727642
C	1.734173309	33.47598777	8.881795756
C	2.130590852	34.55501601	9.900247156
C	1.312382106	34.09679538	7.54180573
N	1.44453495	30.12421376	10.43673297
C	1.485512051	29.34615382	9.197071053
C	0.667974693	30.02250373	8.074529682
O	-0.336170615	30.71817994	8.29714982
C	0.835070358	28.01077929	9.619986756
C	-0.254560878	28.46411071	10.60581792
C	0.394518305	29.64073116	11.35408956
N	1.140671586	29.73389102	6.83967224
C	0.621445401	30.30583497	5.608291688
C	1.718547106	30.3542542	4.542225432
S	2.260924165	28.68492436	3.976514118
H	2.370845155	26.39922506	5.639494309
H	3.961020522	24.92673958	7.058970472
H	3.112180999	24.233313	4.857108183
H	4.824352463	23.80541673	5.06731832
H	4.956140628	23.79419064	2.125479662
H	4.849077979	28.03166825	1.799311631
H	5.260424286	25.83671172	0.588297438
H	7.84124659	27.51373896	6.043357589
H	4.99801156	28.4264423	7.909747264
H	4.39895743	30.4985159	8.422422091

H	3.906755977	32.36986268	10.54787593
H	2.531608145	31.72038408	7.872744731
H	3.734780913	32.96969012	8.194353705
H	0.855478605	32.9208831	9.2800782310
H	3.045046553	35.0934052	9.5689110960
H	2.328145493	34.11042769	10.89533225
H	1.322082867	35.30629684	10.01777357
H	2.15194792	34.66555261	7.086812945
H	0.461247672	34.79652726	7.671771366
H	1.005053584	33.31533563	6.816458114
H	2.525558475	29.20103384	8.854310597
H	1.600143989	27.38863574	10.12897599
H	0.448168014	27.43949406	8.753939087
H	-0.578870299	27.65939277	11.29319819
H	-1.141526614	28.8189232	10.04531382
H	-0.320080693	30.45470078	11.59054699
H	0.865686779	29.33006224	12.31170776
H	2.072584243	29.29099061	6.779023843
H	2.603849758	30.90395426	4.924528537
H	1.336665702	30.88333147	3.646236084
H	3.043386224	27.06278289	6.989998012
H	-0.250122088	29.72270591	5.234418295
H	0.252048747	31.33339733	5.819600401
H	6.718989608	28.76886598	10.34879526
H	5.263683242	27.74889133	10.43752065
C	6.534312533	29.85108201	4.493783682
N	5.253367904	29.49456136	4.095117358

C	7.064265785	30.7014682	3.535298822
N	6.083512663	30.86190789	2.579613477
C	5.00392904	30.12891348	2.942500546
H	4.069795678	30.07050529	2.374465621
H	6.150573058	31.43660553	1.735284837
H	8.104641965	29.87274844	5.938132162
H	6.451828106	30.18994171	6.541189399
H	8.028018981	31.2162979	3.482363774

References.

1) Ellman, G. L. Arch. Biochem Biophys. 1959, 82, 70-77.

2a) Scarrow, R. S.; Shearer, J. EXAFS123, Version 0.5; Trinity University: San Antonio, TX, 2019. 2b) Scarrow, R.C.; Strickler, B.S.; Ellison, J.J.; Shoner, S.C.; Kovacs, J.A.; Cummings, J.G.; Nelson, M.J. J. Am. Chem. Soc., 1998, 120, 9237-9245. 2c) Scarrow, R. C.; Trimitsis, M. G.; Buck, C. P.; Grove, G. N.; Cowling, R. A.; Nelson, M. J. Biochemistry, 1994, 33, 15023-15035. d) Rehr, J.J., Kas, J.J., Vila, F.D., Prange, M.P., Jorissen K., Phys. Chem. Chem. Phys., 2010, 12, 5503-5513.

3) Bunker, G.; Hasnain, S.; Sayers, D. X-ray Absorption Fine Structure; Hasnain, S. S., Ed.; Ellis Horwood: New York, 1991, pp 751-770.

4) Stavitski, E.; de Groot, F. M. F. Micron 2010, 41, 687-694.

5) Rose, K; Shadle, S.E.; Eldsness, M.K.; Kurtz, D.M.; Scott, R.A.; Hedman, B.; Hodgson, K.O.; Solomon, E.I. J. Am. Chem. Soc., 1998, 120, 10743-10747.

6) Neese, F. Wiley Interdiscip. Rev.: Comput. Mol. Sci., 2025, 15, 2, e70019

7) Soda, T.; Kitagawa, Y.; Onishi, T.; Takano, Y.; Shigeta, Y.; Nagao, H.; Yoshioka, Y.; Yamaguchi, K. Chem. Phys. Lett., 2000, 319, 223-230.

8) Pettersen EF, Goddard TD, Huang CC, Couch GS, Greenblatt DM, Meng EC, Ferrin TE. J Comput Chem. 2004, 25, 1605-1612.